Journal of Clinical Monitoring and Computing
https://doi.org/10.1007/s10877-021-00662-8

REVIEW PAPER

# The contemporary pulmonary artery catheter. Part 1: placement and waveform analysis

I. T. Bootsma[1] · E. C. Boerma[1] · F. de Lange[1] · T. W. L. Scheeren[2]

Received: 14 September 2020 / Accepted: 20 January 2021


## Abstract

Nowadays, the classical pulmonary artery catheter (PAC) has an almost 50-year-old history of its clinical use for hemodynamic monitoring. In recent years, the PAC evolved from a device that enabled intermittent cardiac output measurements in combination with static pressures to a monitoring tool that provides continuous data on cardiac output, oxygen supply and-demand balance, as well as right ventricular (RV) performance. In this review, which consists of two parts, we will introduce the difference between intermittent pulmonary artery thermodilution using cold bolus injections, and the contemporary PAC enabling continuous measurements by using a thermal filament which at random heats up the blood. In this first part, the insertion techniques, interpretation of waveforms of the PAC, the interaction of waveforms with the respiratory cycle and airway pressure as well as pitfalls in waveform analysis are discussed. The second part will cover the measurements of the contemporary PAC including measurement of continuous cardiac output, RV ejection fraction, end-diastolic volume index, and mixed venous oxygen saturation. Limitations of all of these measurements will be highlighted there as well. We conclude that thorough understanding of measurements obtained from the PAC are the first step in successful application of the PAC in daily clinical practice.

**Keywords** Hemodynamic monitoring · Pulmonary artery catheter · Waveform characteristics · Pulmonary artery pressure

**Abbreviations**

| | |
|---|---|
| CCO | Continuous cardiac output |
| COPD | Chronic obstructive pulmonary disease |
| CVP | Central venous pressure |
| ECG | Electrocardiogram |
| EDV | End-diastolic volume |
| ICU | Intensive care unit |
| IJV | Internal jugular vein |
| LAP | Left atrial pressure |
| LV | Left ventricle |
| LVEDP | Left ventricular end-diastolic pressure |
| PA | Pulmonary arterial |
| PAC | Pulmonary artery catheter |
| PAOP | Pulmonary artery occlusion pressure |
| PAP | Pulmonary arterial pressure |
| PAWP | Pulmonary artery wedge pressure |
| PEEP | Positive end-expiratory pressure |
| RCT | Randomized controlled trial |
| RV | Right ventricle |
| $ScvO_2$ | Central venous oxygen saturation |
| $SvO_2$ | Mixed venous oxygen saturation |

## 1 Introduction

In 1970 the floating pulmonary artery catheter (PAC) was introduced by Swan and Ganz [1]. The underlying objective of the two physicians was to apply physiologic principles to the understanding of the circulatory abnormalities characterizing an illness in an individual patient, and to provide a rational basis for selection of therapy with objective, quantitative assessment of patient response [1]. The principal stimulus for the development of the PAC was the aim to study and improve the care of acutely ill patients in whom fluoroscopy was not readily available or who were not in a condition to be readily moved to a diagnostic facility [1]. Despite these noble intentions, over time the PAC has predominantly become a topic of debate concerning safety,

✉ I. T. Bootsma
ingebootsma@gmail.com

[1] Department of Intensive Care, Medical Center Leeuwarden, Henri Dunantweg 2, P.O. Box 888. 8901, Leeuwarden, The Netherlands

[2] Department of Anesthesiology, University of Groningen, University Medical Center Groningen, Groningen, The Netherlands

Published online: 10 February 2021

indication and clinical utility, with the main focus on the potential of the PAC to improve clinical patient outcome [2–4]. Fuelled by large randomized controlled trials (RCT) that failed to demonstrate any outcome benefit in relation to PAC-use in a large variety of disease states, the verdict on general application in the clinical setting has become predominantly negative [5–8]. In spite of this the use of PAC's is still widespread, especially in the fields of cardiology and cardiac surgery [9, 10]. This seeming controversy may be due to the understanding of clinicians on the potential limitations of PAC oriented RCT's, including patient selection, timing and the general absence of a protocolized strategy based on PAC-derived variables [5, 11–14]. However, the most probable explanation might be that clinicians from all over the world value the fundamental understanding of physiological principles in the management of complex disease states [15, 16]. In this respect it remains key to acknowledge that adequate interpretation of PAC-derived data requires both skills and knowledge about the correct use of the device, as well as of its pitfalls. The classical PAC evolved from a device that enabled intermittent cardiac output measurements in combination with static pressures to a contemporary PAC, which in turn provided continuous data on cardiac output (CCO-PAC), oxygen supply and demand balance, as well as right ventricular (RV) performance. This CCO-PAC, further mentioned as PAC, is a 7.5 F continuous cardiac output/mixed venous oxygen saturation [$SvO_2$]/continuous end diastolic volume [CEDV]-pulmonary artery catheter (model 774F75; Edwards Lifesciences, Irvine, CA, USA).

The additional information that comes from these technological innovations is specifically included in this review. This narrative review reflects a concise overview of the available knowledge. In the first part of this review, we will discuss catheter placement, waveform characteristics, and pitfalls. In the second part we will describe technical features, clinical applications, limitations, and complications of this contemporary PAC.

## 2 Placement of the pulmonary artery catheter

The PAC is introduced via a dedicated sheath during a sterile procedure using the Seldinger technique. Ultrasound guidance during catheter placement is highly recommended [17, 18]. Placement of the sheath can be into either one of the internal jugular veins (IJV), the subclavian veins, or the femoral veins. The right IJV is the favoured site for sheath placement since it provides the most direct route towards the right ventricle. Although subclavian access is associated with fewer infectious complications compared to femoral or jugular access, bleeding complications may have more serious consequences and anatomical location and vessel size vary considerably [19–21]. Furthermore, ultrasound visualization of the subclavian vein is technically demanding, due to interference by the collarbone [22]. After successful placement of the introducer, the PAC can be inserted through the sheath. The PAC is 110 cm in length, marked at 10 cm intervals, and has at least 2 channels. The distal channel at the tip of the catheter allows for transducing pulmonary artery pressure (PAP) and $SvO_2$ sampling, while the proximal channel is used for measuring central venous pressure (CVP) and central venous saturation ($ScvO_2$) sampling. A balloon is located just below the tip of the catheter, in which 1.5 ml of air can be inflated once the PAC is inserted beyond the sheath (at least 20 cm). Before placement, in vitro calibration of the $SvO_2$ fiberoptic should be performed using a photodetector before removal of the catheter from the package. After calibration, the catheter can be connected to the monitor and transducer. Subsequently, both the proximal and distal channel should be flushed and filled with fluid. In case in vitro calibration of the fiberoptic is not performed, in vivo calibration may be performed after correct placement of the catheter by drawing a blood sample from the distal channel and analysing this sample for $SvO_2$. It is of note that this calibration process is only applicable for the contemporary PAC and not for the older PAC, which obtains cardiac output from intermittent thermodilution. A detailed description on $SvO_2$ can be found in part two of the review.

Placement of the PAC is guided by the characteristics of vascular pressures and waveforms (Fig. 1). In order to facilitate this, the distal lumen of the catheter should be attached to a pressure transducer. Despite individual variety, specific landmarks are well-related to insertion length, depending on the puncture site. After introduction via the right IJV or the right/left subclavian vein, the right atrium should be reached at approximately 20 cm insertion depth; the right ventricle at 30–35 cm, the pulmonary artery at 40–45 cm, and the wedge position at 50 cm (Fig. 1) [23]. For the left IJV one should add 5 cm to each of the previously mentioned landmarks. However, in populations with shorter statures, the insertion length is usually less deep [24]. In case of heart failure with dilatation of the RV, or in tall patients, an insertion length of greater than 50 cm might be necessary. When removing the PAC from its packaging, it has a natural curvature which should be pointed towards the heart. Counter clockwise rotation during insertion with an inflated balloon increases the odds of entering the right atrium and passing the tricuspid valve [25]. When the RV waveform does not appear after 40–45 cm of insertion, or if the PAP waveform does not appear after 50–55 cm, the balloon should be deflated and the catheter should be withdrawn until 20 cm with subsequent repetition of the procedure. To facilitate successful placement of the PAC, positioning

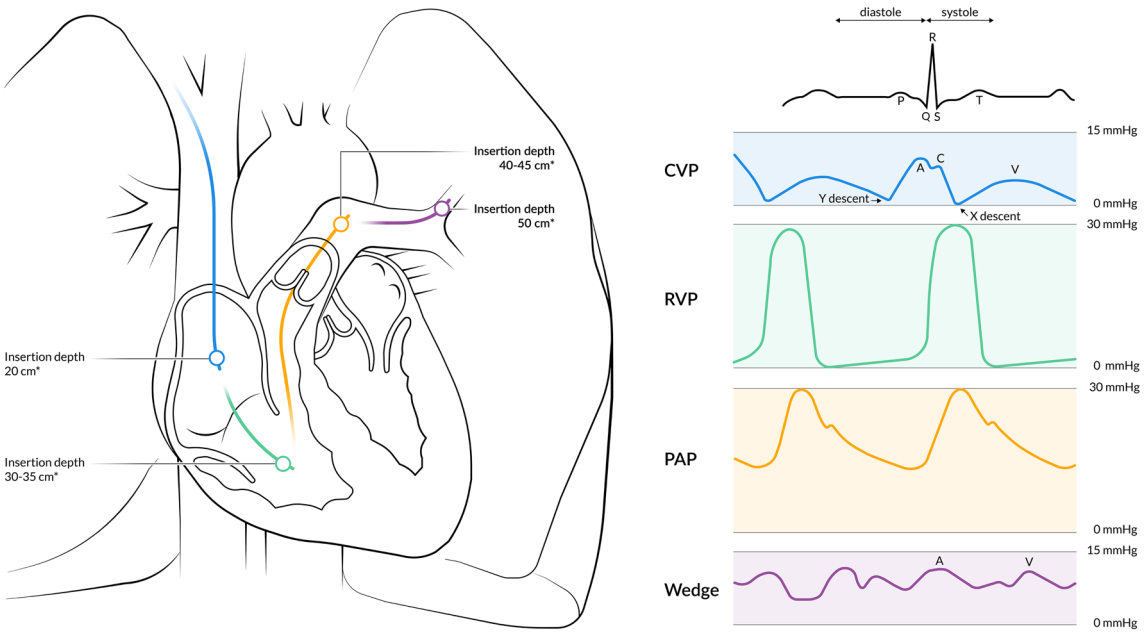


**Fig. 1** Placement of the PAC guided by the characteristics of normal vascular pressures and waveforms . *For placement in the left internal jugular vein or left subclavian vein one should add 5 cm to each of the landmarks . *CVP* central venous pressure, *PAC* pulmonary artery catheter, *PAP* pulmonary artery pressure, *RVP* right ventricular pressure

the patient head-down will aid flotation past the tricuspid valve. In order to facilitate the passage through the pulmonary valve, positioning the operation table or ICU bed with head up (15°–20°) and rotated to the right may be helpful [23, 26]. Most catheters float easily toward the right pulmonary artery catheter. In order to selectively catheterize the left pulmonary artery, the patient should be positioned with the right side down. In the setting of low cardiac output, deep inspiration in non-intubated, spontaneously breathing patients will increase right ventricular output transiently and therefore may facilitate catheter flotation [23]. After correct placement, in vivo calibration of the fiberoptic should be performed.

## 2.1 Zeroing

Zeroing and leveling of the catheter are a prerequisites to obtaining accurate measurements, and both have revealed to be susceptible to error [27]. Opening the stopcock to ambient air, the hemodynamic monitoring system will be exposed to atmospheric pressure. After pressing 'zeroing' on the monitor and confirming the calibration, the transducer stopcock can be turned back into its original position. The atmospheric pressure is now the zero-reference point. From there on, only (variations in) pressures which exist inside the heart chamber or blood vessel will be measured, as long as the position of the pressure transducer remains the same [28].

## 2.2 Leveling

The main goal of leveling the external transducer is to eliminate additional hydrostatic pressure from the fluid column. This hydrostatic pressure is proportional to the height of the fluid column. The level of the transducer should be even with the top of the fluid column in the chamber or vessel in which the pressure is to be measured [29]. The correct position in supine patients is the phlebostatic axis, which is about 5 cm below the sternal angle [30]. When patients are in prone or sitting position reference levels might be different [31]. In case the transducer is placed above the phlebostatic axis, the pressure will be underestimated. Vice versa, the measured pressure will be erroneously high in case the transducer is placed below the phlebostatic axis.

## 2.3 Waveforms of the pulmonary artery catheter

### 2.3.1 Central venous/right atrial pressure waveform

Initially, the PAC is passed through the introducer sheath until it reaches the IJV, the superior vena cava, and the right atrium. Reaching this point, the monitor will depict either a CVP or right atrial pressure waveform, which are considered to be identical. A normal CVP waveform consists of

5 phases; three peaks (a-wave: atrial contraction; c-wave: isovolumic ventricular contraction, tricuspid motion toward right atrium; v-wave: systolic filling of the atrium), and two troughs (x: atrial relaxation; y: early ventricular filling). Identification of CVP waveform components is facilitated by aligning the pressure waveform with the ECG trace. The a-wave follows the ECG P-wave, the c-wave always follows the ECG R-wave and the v-wave follows the ECG T-wave [32]. CVP should be measured at the base of the c-wave, just after the R-wave of the ECG, because this represents the final pressure in the ventricle before onset of the systole. If the c-wave is not identified and the patient has sinus rhythm, the base of the a-wave can be used. A normal CVP range in healthy, spontaneously breathing humans in the supine position is between 0 and 10 mmHg (Fig. 1) [33].

#### 2.3.2 Right ventricular pressure waveform

When advancing the PAC with an inflated balloon through the tricuspid valve, RV pressures will be recorded. The major difference with the CVP characteristics is a marked increase in systolic RV pressure. A normal RV-waveform is characterized by a steep, rapid systolic slope. Due to the substantial compliance of the normal RV, the diastolic slope is typically horizontal [34, 35]. Diastolic pressure in the RV of a healthy individual is almost equal to zero. End diastolic pressure is measured right before the R-wave on the ECG, before the beginning of the systolic upslope [34]. Normal systolic pressure of the RV ranges between 15 and 28 mmHg (Fig. 1).

#### 2.3.3 Pulmonary artery pressure waveform

By advancing the catheter further with the use of an inflated balloon, the PAC will float across the pulmonary valve into the pulmonary artery, displaying a PAP waveform. The most distinctive feature in comparison to the RV pressure waveform is the increment in diastolic pressure in the pulmonary artery compared to the diastolic pressure in the normal RV (Fig. 2a). This is otherwise known as the diastolic pressure step up [23]. It is of note that this diastolic pressure step up can be minimal in the setting of right heart failure. The PAP waveform consists of 4 phases, the first being a steep, rapid systolic upstroke, which is followed by a systolic peak. In a normal PAP waveform, there should be no significant pressure difference between the peak systolic RV pressure and peak systolic PAP. The normal gradient between systolic RV and PAP is 0 to 3 mmHg [36, 37]. The third phase is the dicrotic notch, which represents the closure of the pulmonary valve, and thus the beginning of the diastole. The dicrotic notch always follows the T-wave of the ECG. After the dicrotic notch comes the diastolic run-off, which marks the diastolic phase of the waveform. Normal systolic PAP ranges between 14 and 28 mmHg, normal diastolic PAP ranges between 5 and 16 mmHg, and normal mean PAP between 10 and 22 mmHg (Fig. 1).

#### 2.3.4 Wedge position

After further insertion the PAC will finally reach its wedge position. Balloon occlusion stops all distal flow and creates a static fluid column between the tip of the catheter and the junction point of the pulmonary veins and left atrium. The pulmonary artery wedge pressure (PAWP) is believed to reflect both the pressures in the pulmonary veins as well as in the left atrium [38]. In general, PAWP and pulmonary artery occlusion pressure (PAOP) can be used interchangeably and both refer to the same measurement. The PAWP waveform usually depicts two pressure peaks: the a-wave and the v-wave, as well as two descents called x and y. The v-wave is generally the most prominent peak. The c-wave is often difficult to discern in a normal wedge pressure trace due to the delayed representation of the left atrial pressure, the damped reflection, and a shorter time interval between atrial and ventricular contraction of the left atrium compared to that of the right atrium [39]. It is important to keep in mind that the PAWP is a delayed representation of the left atrial pressure since the pulmonary vascular bed is positioned between the PAC and the left atrium. In addition, PAWP is also a damped reflection of phasic atrial pressure waves. The amount of damping is variable; however pressure peaks can potentially be significantly underestimated [40]. As a result of this time lag, the a-wave of the wedge pressure will be visualized shortly after the R-wave on the ECG, although the a-wave represents the end-diastolic phase [39]. Since the wedge position of the balloon does not stop flow in the antegrade direction completely, PAWP is always lower than the mean PAP. After reaching the wedge position the balloon should be deflated and not advanced any further. After deflating the balloon, the PAP waveform should re-appear. If not, the catheter should be retracted for about 2 cm. PAWP should be measured at the end of the a-wave or before the QRS complex, at the end of the expiration, when pleural pressures are minimal, and should ideally be recorded as the mean of three measurements. However, most devices provide digitized mean PAWP. A normal PAWP range is between 5 and 12 mmHg (Fig. 1) [41].

### 2.4 Interaction with waveforms

#### 2.4.1 Catheter position

In the human lung there are 3 vertical zones, called the West zones, each with a different physiology. In West zone 1 (apex), alveolar pressure exceeds the pulmonary artery and pulmonary venous pressures. In West zone 2 (central),

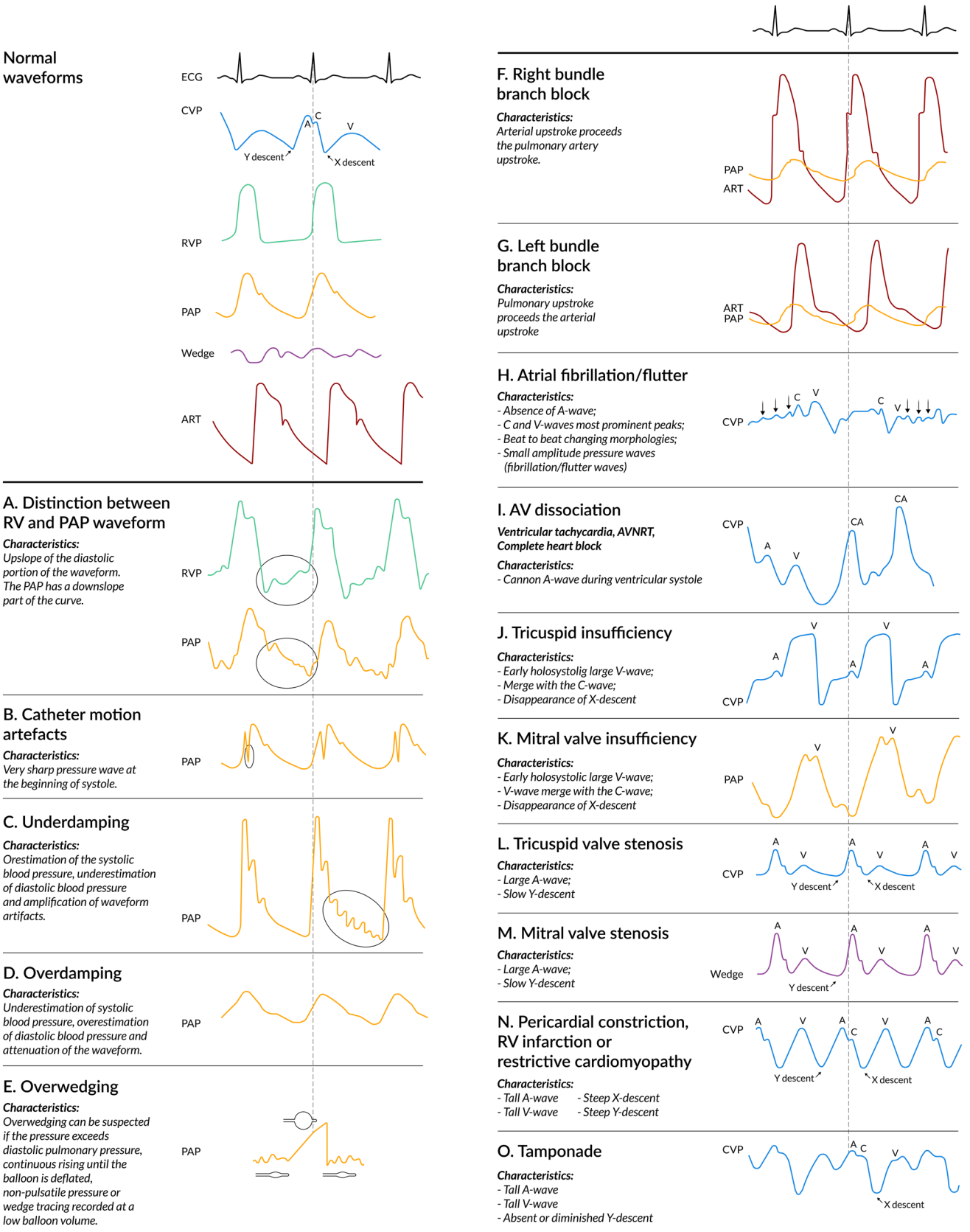


**Fig. 2** Pressure waveform pitfalls and abnormalities . *CA* cannon a-wave, *CVP* central venous pressure, *ECG* electrocardiogram, *RV* right ventricle, *RVP* right ventricular pressure, *PAP* pulmonary artery pressure, *ART* arterial

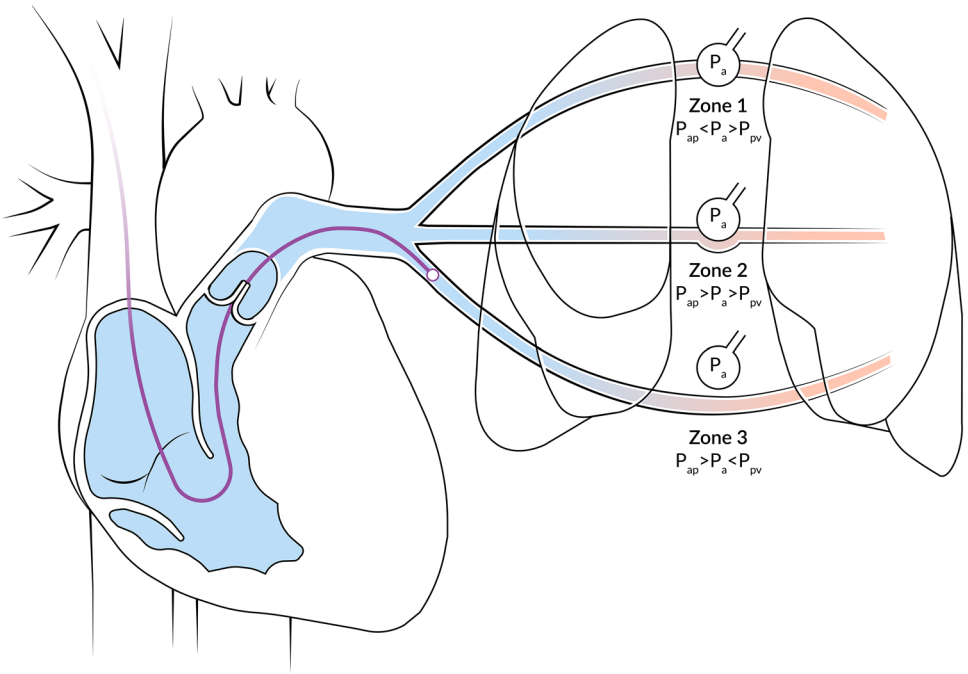


**Fig. 3** Pulmonary artery catheter location in relationship to West`s zones of the lung $P_{ap}$ **pulmonary** arterial pressure, $P_a$ pressure in the alveoli, $P_{pv}$ pulmonary venous pressure

the alveolar pressure exceeds only the pulmonary venous pressure, and in West zone 3 (base) the alveolar pressure is lower than both the arterial and venous pulmonary pressures (Fig. 3) [42]. When the alveolar pressure exceeds the pulmonary vein pressure in West zone 1 or 2, the pressure derived at the tip of the PAC is the alveolar pressure instead of pulmonary venous pressure (or left atrial pressure; LAP or left ventricular end-diastolic pressure; LVEDP). Therefore, positioning the tip of the PAC and measurement in West zone 3 is a prerequisite for PAWP to accurately reflect LAP (Fig. 3). Absent a and v-waves, marked as PAWP variation during the respiration cycle, and pulmonary artery diastolic pressure exceeding wedge pressure (in the absence of tall a or v-waves) can indicate an incorrect wedge position in West zone 1 or 2 [43].

#### 2.4.2 Respiratory cycle

CVP, PAP, and PAWP values should be measured at the end of expiration. At this point, the pleural pressure is closest to atmospheric pressure, and thus the influence of pleural pressures on measurements which are being compared to atmospheric pressure is minimal, both during spontaneous and positive pressure ventilation. Exceptions from this rule are spontaneously breathing COPD patients with forced expiration, where CVP should be measured early in expiration, before the patient begins to push. One should be aware of the fact that this may not necessarily be the highest or lowest pressure measured during the respiratory cycle [44].

#### 2.4.3 Airway pressure

Positive end-expiratory pressure (PEEP), either intrinsic or extrinsic, can influence measured pressures by its effect on pericardial pressure. During spontaneous breathing, and even during positive pressure ventilation with zero end-expiratory pressure, the pericardial pressure is minimal at the end of expiration. With PEEP applied, the pericardial pressure exceeds zero and can lead to overestimation of LVEDP and CVP [33, 38]. Therefore, CVP and PAWP might not be true indications of LAP when a patient is receiving a PEEP of 10 $cmH_20$ or more [45]. Different methods to correct for applied PEEP are suggested, including various formulas or abrupt airway disconnection [45–48]. An often used formula is: corrected pressure (mmHg) = measured pressure (mmHg) – [0.5x (PEEP/1.36)] [49]. Awareness of possible overestimation of PAWP due to PEEP from various lung compliance during mechanical ventilation is critical in the correct interpretation of the data.

### 2.5 Waveform pitfalls

The most common artefact is the catheter whip [50]. At the onset of systole, the catheter may be set into motion by closure of the tricuspid valve and by RV contraction. Fluid within the catheter might accelerate due to the movement of the catheter, or the catheter might strike either the walls of the heart or pulmonary artery. In the waveform, a very sharp pressure wave will appear at the beginning of systole (just after the R-wave of the ECG) and will only be visible in the RV and PAP tracing (Fig. 2b). This will not only result in a

waveform artefact but also in artefactual pressure peaks [51]. Repositioning of the catheter with 1 or 2 centimetres may be helpful when trying to obtain more accurate pressures. It is of note that, although it might result in more accurate pressures, the artefact will probably still be visible.

#### 2.5.1 Damping

Catheter-transducer monitoring systems have three characteristic physical properties: elasticity, mass, and friction. These properties determine the system's operating characteristics, referred to as the dynamic response. An optimal dynamic response is required to measure pressures accurately. The dynamic response is characterized by both the natural frequency and the damping coefficient. The natural frequency describes how rapidly the system oscillates and the damping coefficient describes how rapidly it comes to rest [52]. The fast-flush test has been invented in order to evaluate the dynamic bedside response by briefly giving a fast flush several times, preferably during the diastolic pressure run-off [53]. The clinician should observe the natural frequency by counting the distance between oscillations, and the damping coefficient by counting how quickly the systems returns to baseline. In an optimally damped waveform, 1.5 to 2 oscillations are seen. When there are more oscillations, the system is underdamped; when there are less, the system is overdamped. An underdamped system will overestimate the systolic blood pressure and/or underestimate diastolic blood pressure, which will result in amplification of waveform artifacts (Fig. 2c). Overdamped systems will underestimate systolic blood pressure and/or overestimate diastolic blood pressure (Fig. 2d) [53]. Due to the intrinsic properties of the monitoring set-up, waveform analysis at high heart rates might be unreliable and difficult to execute.

Failure to remove all air from the catheter or tubing, or obstruction of the pressure channel of the catheter by blood clots, might result in overdamping of the waveform, which would lead to falsely low systolic pressure measurements. In case of an underdamped system, it is not advised to introduce a small air bubble into the tubing. By adding an air bubble the natural frequency of the system will be lower, resulting in further amplifying systolic pressure overshoot [53]. A clinician should be aware of artefacts producing erroneous values on the monitor. This can be the result of artefactual pressure troughs, resulting in nadir pressures that are recorded as diastolic pressures but which are not the factual diastolic pressure. Advancing or withdrawing the catheter might be helpful when removing the artefact and replace the pressure with a more accurate measurement of the diastolic pulmonary artery pressure [52]. In the event that overdamping or underdamping cannot be corrected, the clinician may consider replacing the catheter. If this is impossible or undesirable, the clinician should not use the absolute values of systolic and/or diastolic PAP for the correct interpretation of the clinical situation. However, the trend of these variables over time may still reflect actual hemodynamic changes.

#### 2.5.2 Elevated right ventricular pressures

In case end-diastolic pressure of the RV is elevated, as in RV failure, it might be difficult to distinguish RV pressure from PAP. Close examination of the diastolic component of the waveform is likely to reveal the answer, since a diastolic step up is limited in the setting of right heart failure. The PAP is always going to decrease during the diastolic phase (after the dicrotic notch), as blood flows toward the left atrium, whereas the pressure in the RV steadily increases during diastole due to filling of the RV. In addition, the RV waveform can also depict a notch, called the incisura, caused by closure of the pulmonic valve. However, this notch will originate simultaneously with the T-wave instead of after the T-wave, as is the case with the dicrotic notch of the PAP waveform (Fig. 2a) [23]. Analysis of the RV waveform can be useful in early detection and subsequent management of RV dysfunction, especially during cardiac surgery [35, 54]. Under conditions of impaired RV function, the diastolic slope may change. In the early stage of RV failure, the diastolic phase is characterized by a progressively oblique upslope. During severe impaired RV function the diastolic RV waveform will become square-root shaped. In addition, elevated systolic pressures have been described in the setting of RV outflow tract obstruction. This condition, defined as a pressure gradient between RV and PAP of at least 25 mmHg, can happen in up to 4% of cardiac surgery patients and is associated with hemodynamic instability [37]. Since RV pressure monitoring requires a different PAC with a dedicated RV pace-port, further details are beyond the scope of this review. An excellent review of this topic is provided by Raymond and colleagues [35]. It is of note that the PAC used for RV pressure monitoring does not enable continuous cardiac output and RV ejection fraction measurements.

#### 2.5.3 Overwedging and underwedging

Overwedging occurs when eccentric balloon inflation causes the catheter tip to occlude against the pulmonary artery wall, after which it thus no longer measures intravascular pressure. Instead, pressure is now produced by a pressurized continuous flush system as it builds up against obstructed distal opening. Overwedging can be suspected under any of the following circumstances: if the pressure exceeds diastolic pulmonary pressure, if the waveform continuously rises until the balloon is deflated, if the pressure is non-pulsatile, and/or if wedge tracing is recorded at a low balloon volume

(< 1.5 cc) (Fig. 2e). Since overwedging is mostly caused by distal migration of the catheter, the solution is usually to withdraw the PAC to a more proximal position [51]. It is of note that inflation of the balloon, while the catheter is migrated to a distal position, should be avoided because it may cause rupture of a small pulmonary vessel, which can lead to serious lung hemorrhage. In patients with high PAP, underwedging can occur from incomplete occlusion of the pulmonary artery branch, which is related to poor compliance of the pulmonary arteries and will lead to an overestimation of the PAWP [55].

## 2.6 Waveform abnormalities

Several clinical pathologies can have impact on PA waveform appearances. All described clinical conditions and their corresponding waveforms can be found in Fig. 2.

### 2.6.1 Heart rhythms and bundle branch blocks

When interpreting waveforms, simultaneous observation of pulmonary artery waveforms with the ECG registration and with arterial waveform monitoring could be useful. Under normal conditions, the PAP upstroke precedes the arterial upstroke due to the longer duration of left ventricular isovolumetric contraction [56]. Since this lag time is small under normal conditions, the waveforms may seem to overlap. However, the presence of a bundle branch block may alter this relation between PAP and systemic arterial pressure. A left bundle branch block delays left ventricular contraction, increasing the lag time between the PAP upstroke and arterial upstroke even more (Fig. 2g). A right bundle branch block has the opposite effect; arterial upstroke now precedes PAP upstroke (Fig. 2f) [23]. Tachycardia might produce fusion of waveform components, particularly the a and c-waves, whereas bradycardia can reveal a mid-diastolic plateaus pressure wave (h) between the x-descent and v-peak [57]. In case of atrial fibrillation, the a-wave will disappear from the CVP waveform due to the loss of atrial contraction. The c-wave is more prominent compared to normal sinus rhythm due to high end-diastolic atrial volume and subsequent isovolumetric ventricular contraction, displacing the tricuspid valve toward the right atrium. Atrial fibrillation leads to variability in chamber filling, and thereby to the contractile state with concurrent changes in waveform morphologies. In addition to the c- and v-waves, small amplitude pressure waves may be superimposed to the waveform, reflecting atrial activity (Fig. 2h) [57, 58]. In case of atrioventricular dissociation (ventricular tachycardia, complete heart block, re-entry tachycardia), cannon a-waves are inscribed in the CVP waveform because of atrial contraction against a closed tricuspid valve during systole. Cannon a-waves may occur before, during, or after the c-wave. Cannon a-waves can also be noted in the wedge pressure waveform (Fig. 2i) [59].

### 2.6.2 Tricuspid valve disease

In case of severe tricuspid regurgitation, blood leaks back from the RV towards the right atrium across the incompetent valve. This will result in an early systolic large v-wave on the CVP waveform. Since this v-wave is holosystolic, it will merge with the c-wave and make the x-descent disappear (Fig. 2j) [60]. Tricuspid stenosis causes an obstruction between the right atrium and the RV, resulting in diminished right atrial emptying, impaired RV filling, and elevation of mean CVP. Tricuspid stenosis affects the diastolic portion of the CVP; the waveform will depict a prominent a-wave and a slow y-descent (Fig. 2l). Other diseases which impair RV filling by increasing RV stiffness (RV infarction, pericardial constriction, pulmonic stenosis, pulmonary hypertension) may produce a prominent end-diastolic a-wave and a taller v-wave, but the y-descent should be preserved [57, 58].

### 2.6.3 Mitral valve disease

Mitral valve regurgitation has similar implications for the PAP/PAWP waveform as the previously described tricuspid regurgitation has for the CVP waveform. The holosystolic prominent v-wave with fusion of the c-wave and obliteration of the x-descent will define the PAP and PAWP waveform in the presence of mitral valve regurgitation (Fig. 2k). However, due to the delayed, damped reflection of the left atrial pressure, c-wave merging can be less evident [60]. It is of note that the height of the v-waves does not predict the intensity of the mitral valve regurgitation [61]. The presence of a large v-wave in PAWP waveforms may complicate a true distinction between PAWP and PAP waveform. In case this happens, drawing a comparison with the ECG and arterial waveform may be helpful. The PAWP will start after both the arterial upstroke and the T-wave on the ECG, while the PAP will slightly precede both systemic arterial pressure upstroke and the T-wave [62]. Like tricuspid stenosis in the CVP waveform, the PAWP waveform will depict a prominent end-diastolic a-wave, and a slow y-descent in case of mitral valve stenosis (Fig. 2m). Increased LV stiffness (left ventricular infarction and hypertrophy, pericardial constriction, aortic stenosis, and systemic arterial hypertension) will produce a prominent a-wave, but the y-descent should be preserved [60].

### 2.6.4 Restrictive physiology

In pericardial constriction, the PAP waveform is markedly different. All of the waveform components are amplified; tall a and v-waves with steep x and y-descents are visible,

creating a sawtooth M (in case of a fast heart rate) or W configuration (in case of a slow heart rate) [58]. These morphologic features may also be seen in the CVP waveform of patients with RV infarction or restrictive cardiomyopathy, since both pathologic conditions share the same underlying pathophysiologic mechanisms (Fig. 2n) [63, 64].

#### 2.6.5 Cardiac tamponade

Compression of the heart due to pericardial fluid results in an increased CVP, as well as in a reduced cardiac diastolic volume, stroke volume, and cardiac output. Despite the hemodynamic similarities between pericardial constriction and tamponade, the PAP waveform is slightly different [65]. The characteristic of the CVP waveform in cardiac tamponade is monophasic and dominated by a systolic x-descent. The y-descent is diminished, or altogether absent, due to impaired RV filling (Fig. 2o) [58]. This is caused by the difference in blood flow from the vena cava to the right atrium between pericardial constriction and tamponade. In cardiac tamponade, venous return to the right atrium is limited to the period of atrial relaxation (x-descent), whereas in restrictive pathophysiology, it is biphasic with a peak during atrial relaxation and early ventricular filling (x- and y-descent) [65].

#### 2.6.6 Left ventricular end diastolic pressure

According to the principle of communicating tubes, the PAWP may be used as an indicator of LV filling pressure (LVEDP). The mitral valve is open at the end of diastole and thus, to some extent, PAWP represents the pressure in the left atrium and LV as well. However, these pressures are not necessarily the same. The LVEDP determines the force of ventricular contraction, whereas the mean left atrial pressure is the pressure level which, on average, must be exceeded if blood is to return to the heart [66]. The true filling pressure is the net result of the intracavitary LVEDP and the transmural pressure. Therefore, pericardial pressures (or juxtacardiac pressures) and mediastinal pressures should be taken into account. Under normal conditions, these pressures are respectively zero and between −1 and −3 mmHg, and thus PAWP is assumed to accurately reflect LVEDP [67]. However, in certain specific pathophysiological situations, measurements of PAWP do not accurately reflect LVEDP due to changes in pericardial or mediastinal pressures. Underestimation can occur during diminished LV compliance, in case of obstruction of pulmonary blood flow, during aortic or pulmonic valve regurgitation, or during right bundle branch block. Overestimation can be caused by positive end-expiratory pressure, pulmonary veno-occlusive disease, pulmonary arterial hypertension, mitral valve stenosis or regurgitation, tachycardia, or ventricular septal defect [43].

## 3 Conclusions

Adequate catheter placement and detailed understanding of PAC-derived waveform characteristics are a prerequisite for the correct interpretation of physiology and pivotal in clinical decision making. In the second part of this review, we will describe technical features, clinical applications, limitations, and complications of the contemporary PAC.

**Author contributions** All authors contributed to the design of the review. Literature search and data analysis was performed by ITB. The first draft of the manuscript was written by ITB. All authors critically revised the review. All authors read and approved the final manuscript.

## Compliance with ethical standards

**Conflict of interest** ITB, ECB, and FdL do hereby declare that there are no conflict of interest. TWLS received research Grants and honoraria from Edwards Lifesciences (Irvine, CA, USA) and Masimo Inc. (Irvine, CA, USA) for consulting and lecturing and from Pulsion Medical Systems SE (Feldkirchen, Germany) for lecturing. TWLS is editor in chief of the Journal of Clinical Monitoring and Computing but had no role in the handling of this manuscript.

**Ethical approval** Not applicable.

**Informed consent** Not applicable.



## References

1. Swan HJ, Ganz W, Forrester J, Marcus H, Diamond G, Chonette D. Catheterization of the heart in man with use of a flow-directed balloon-tipped catheter. N Engl J Med. 1970;283(9):447–51.
2. Gore JM, Goldberg RJ, Spodick DH, Alpert JS, Dalen JE. A community-wide assessment of the use of pulmonary artery catheters in patients with acute myocardial infarction. Chest. 1987;92(4):721–7.
3. Zion MM, Balkin J, Rosenmann D, Goldbourt U, Reicher-Reiss H, Kaplinsky E, et al. Use of pulmonary artery catheters in patients with acute myocardial infarction. Analysis of experience in 5,841 patients in the SPRINT Registry. SPRINT Study Group. Chest. 1990;98(6):1331–5.
4. Connors AF, Speroff T, Dawson NV, Thomas C, Harrell FE, Wagner D, et al. The effectiveness of right heart catheterization in

the initial care of critically ill patients. SUPPORT Investigators JAMA. 1996;276(11):889–97.
5. Harvey S, Harrison DA, Singer M, Ashcroft J, Jones CM, Elbourne D, et al. Assessment of the clinical effectiveness of pulmonary artery catheters in management of patients in intensive care (PAC-Man): a randomised controlled trial. Lancet. 2005;366(9484):472–7.
6. National Heart Lung and Blood Institute Acute Respiratory Distress Syndrome (ARDS) Clinical Trials Network. Wheeler AP, Bernard GR, Thompson BT, Schoenfeld D, Wiedemann HP, et al. Pulmonary-artery versus central venous catheter to guide treatment of acute lung injury. N Engl J Med. 2006;354(21):2213–24.
7. Sandham JD, Hull RD, Brant RF, Knox L, Pineo GF, Doig CJ, et al. A randomized, controlled trial of the use of pulmonary-artery catheters in high-risk surgical patients. N Engl J Med. 2003;348(1):5–14.
8. Hadian M, Pinsky MR. Evidence-based review of the use of the pulmonary artery catheter: impact data and complications. Crit Care. 2006;10(Suppl 3):8.
9. Binanay C, Califf RM, Hasselblad V, O'Connor CM, Shah MR, Sopko G, et al. Evaluation study of congestive heart failure and pulmonary artery catheterization effectiveness: the ESCAPE trial. JAMA. 2005;294(13):1625–33.
10. Rajaram SS, Desai NK, Kalra A, Gajera M, Cavanaugh SK, Brampton W, et al. Pulmonary artery catheters for adult patients in intensive care. Cochrane Database Syst Rev. 2013;2:CD003408.
11. Greenberg SB, Murphy GS, Vender JS. Current use of the pulmonary artery catheter. Curr Opin Crit Care. 2009;15(3):249–53.
12. Chittock DR, Dhingra VK, Ronco JJ, Russell JA, Forrest DM, Tweeddale M, et al. Severity of illness and risk of death associated with pulmonary artery catheter use. Crit Care Med. 2004;32(4):911–5.
13. Yeh RW, Valsdottir LR, Yeh MW, Shen C, Kramer DB, Strom JB, et al. Parachute use to prevent death and major trauma when jumping from aircraft: randomized controlled trial. BMJ. 2018;363:k5094.
14. Friese RS, Shafi S, Gentilello LM. Pulmonary artery catheter use is associated with reduced mortality in severely injured patients: a National Trauma Data Bank analysis of 53,312 patients. Crit Care Med. 2006;34(6):1597–601.
15. Sotomi Y, Sato N, Kajimoto K, Sakata Y, Mizuno M, Minami Y, et al. Impact of pulmonary artery catheter on outcome in patients with acute heart failure syndromes with hypotension or receiving inotropes: from the ATTEND Registry. Int J Cardiol. 2014;172(1):165–72.
16. Ospina-Tascón GA, Cordioli RL, Vincent JL. What type of monitoring has been shownto improve outcomes in acutely ill patients? Intensive Care Med. 2008;34(5):800–20.
17. Saugel B, Scheeren TWL, Teboul JL. Ultrasound-guided central venous catheter placement: a structured review and recommendations for clinical practice. Crit Care. 2017;21(1):1123.
18. Hind D, Calvert N, McWilliams R, Davidson A, Paisley S, Beverley C, et al. Ultrasonic locating devices for central venous cannulation: meta-analysis. BMJ. 2003;327(7411):361.
19. Ruesch S, Walder B, Tramèr MR. Complications of central venous catheters: internal jugular versus subclavian access–a systematic review. Crit Care Med. 2002;30(2):454–60.
20. Parienti JJ, Mongardon N, Mégarbane B, Mira JP, Kalfon P, Gros A, et al. Intravascular complications of central venous catheterization by insertion site. N Engl J Med. 2015;373(13):1220–9.
21. Lavallée C, Ayoub C, Mansour A, Lambert J, Lebon JS, Lalu MM, et al. Subclavian and axillary vessel anatomy: a prospective observational ultrasound study. Can J Anaesth. 2018;65(4):350–9.
22. Fragou M, Gravvanis A, Dimitriou V, Papalois A, Kouraklis G, Karabinis A, et al. Real-time ultrasound-guided subclavian vein cannulation versus the landmark method in critical care patients: a prospective randomized study. Crit Care Med. 2011;39(7):1607–12.
23. Mark JB. Pulmonary artery pressure. Atlas of cardiovascular monitoring. New York: Churchill Livingstone; 1998. p. 26–37.
24. Tempe D, Gandhi A, Datt V, Gupta M, Tomar A, Rajesh V, et al. Length of insertion for pulmonary artery catheters to locate different cardiac chambers in patients undergoing cardiac surgery. Br J Anaesth. 2006;97(2):147–9.
25. Cronin B, Robbins R, Maus T. Pulmonary artery catheter placement using transesophageal echocardiography. J Cardiothorac Vasc Anesth. 2017;31(1):178–83.
26. Szabó Z. A simple method to pass a pulmonary artery flotation catheter rapidly into the pulmonary artery in anaesthetized patients. Br J Anaesth. 2003;90(6):794–6.
27. Parviainen I, Jakob SM, Suistomaa M, Takala J, Scandinavian Society of Anaesthesiology and Intensive Care Medicine (SSAI). Practical sources of error in measuring pulmonary artery occlusion pressure: a study in participants of a special intensivist training program of The Scandinavian Society of Anaesthesiology and Intensive Care Medicine (SSAI). Acta Anaesthesiol Scand. 2006;50(5):600–3.
28. Quaal SJ. Improving the accuracy of pulmonary artery catheter measurements. J Cardiovasc Nurs. 2001;15(2):71–82.
29. Courtois M, Fattal PG, Kovács SJ, Tiefenbrunn AJ, Ludbrook PA. Anatomically and physiologically based reference level for measurement of intracardiac pressures. Circulation. 1995;92(7):1994–2000.
30. Winsor T, Burch GE. Phlebostatic axis and phlebostatic level, reference levels for venous pressure measurements in man. Proc Soc Exp Biol Med. 1945;58(2):165–9.
31. Song IK, Park HS, Lee JH, Kim EH, Kim HS, Bahk JH, et al. Optimal level of the reference transducer for central venous pressure and pulmonary artery occlusion pressure monitoring in supine, prone, and sitting position. J Clin Monit Comput. 2017;31(2):381–6.
32. Mark JB. Central venous pressure, left atrial pressure. Atlas of cardiovascular monitoring. New York: Churchill Livingstone; 1998. p. 15–25.
33. Magder S. Central venous pressure monitoring. Curr Opin Crit Care. 2006;12(3):219–27.
34. Denault A, Lamarche Y, Rochon A, Cogan J, Liszkowski M, Lebon JS, et al. Innovative Approaches in the perioperative care of the cardiac surgical patient in the operating room and intensive care unit (1). Can J Cardiol. 2014;30(12):459–77.
35. Raymond M, Grønlykke L, Couture EJ, Desjardins G, Cogan J, Cloutier J, et al. Perioperative right ventricular pressure monitoring in cardiac surgery. J Cardiothorac Vasc Anesth. 2019;33(4):1090–104.
36. Gómez CM, Palazzo MG. Pulmonary artery catheterization in anaesthesia and intensive care. Br J Anaesth. 1998;81(6):945–56.
37. Denault AY, Chaput M, Couture P, Hébert Y, Haddad F, Tardif JC. Dynamic right ventricular outflow tract obstruction in cardiac surgery. J Thorac Cardiovasc Surg. 2006;132(1):43–9.
38. O'Quin R, Marini JJ. Pulmonary artery occlusion pressure: clinical physiology, measurement, and interpretation. Am Rev Respir Dis. 1983;128(2):319–26.
39. Mark JB. Pulmonary artery wedge pressure. Atlas of cardiovascular monitoring. New York: Churchill Livingstone; 1998. p. 39–48.
40. Kern MJ, Deligonul U. Interpretation of cardiac pathophysiology from pressure waveform analysis: the left-sided V wave. Cathet Cardiovasc Diagn. 1991;23(3):211–8.

41. Hoeper MM, Bogaard HJ, Condliffe R, Frantz R, Khanna D, Kurzyna M, et al. Definitions and diagnosis of pulmonary hypertension. J Am Coll Cardiol. 2013;62(25):D42-50.
42. West JB, Dollery CTNA. Distribution of blood flow in isolated lung; relation to vascular and alveolar pressures. J Appl Physiol. 1964;19:713–24.
43. Mark JB. Predicting left ventricular end-diastolic pressure. Atlas of cardiovascular monitoring. New York: Churchill Livingstone; 1998. p. 59–79.
44. Respiratory-Circulatory Interactions. Atlas of cardiovascular monitoring. New York: Churchill Livingstone; 1998. p. 261–85.
45. Pinsky M, Vincent JL, De Smet JM. Estimating left ventricular filling pressure during positive end-expiratory pressure in humans. Am Rev Respir Dis. 1991;143(1):25–31.
46. Teboul JL, Pinsky MR, Mercat A, Anguel N, Bernardin G, Achard JM, et al. Estimating cardiac filling pressure in mechanically ventilated patients with hyperinflation. Crit Care Med. 2000;28(11):3631–6.
47. Carter RS, Snyder JV, Pinsky MR. LV filling pressure during PEEP measured by nadir wedge pressure after airway disconnection. Am J Physiol. 1985;249(4 Pt 2):H770-6.
48. Teboul JL, Zapol WM, Brun-Buisson C, Abrouk F, Rauss A, Lemaire F. A comparison of pulmonary artery occlusion pressure and left ventricular end-diastolic pressure during mechanical ventilation with PEEP in patients with severe ARDS. Anesthesiology. 1989;70(2):261–6.
49. Raoof S, Khan FA, editors. Mechanical ventilation manual. Philadelphia: American College of Physicians, 1998.
50. Schmitt EA, Brantigan CO. Common artifacts of pulmonary artery and pulmonary artery wedge pressures: recognition and interpretation. J Clin Monit. 1986;2(1):44–52.
51. Mark JB. Pulmonary artery and wedge pressure artifacts. Atlas of cardiovascular monitoring. New York: Churchill Livingstone; 1998. p. 49–58.
52. Mark JB. Technical requirements for direct blood pressure measurement. Atlas of cardiovascular monitoring. Churchill Livingstone: New York; 1998. p. 98–126.
53. Gardner RM. Direct blood pressure measurement–dynamic response requirements. Anesthesiology. 1981;54(3):227–36.
54. Grønlykke L, Couture EJ, Haddad F, Amsallem M, Ravn HB, Raymond M, et al. Preliminary experience using diastolic right ventricular pressure gradient monitoring in cardiac surgery. J Cardiothorac Vasc Anesth. 2020;34(8):2116–25.
55. Rosenkranz S, Preston IR. Right heart catheterisation: best practice and pitfalls in pulmonary hypertension. Eur Respir Rev. 2015;24(138):642–52.
56. Braunwald E, Fishman AP, Cournand A. Time relationship of dynamic events in the cardiac chambers, pulmonary artery and aorta in man. Circ Res. 1956;4(1):100–7.
57. Mark JB. Getting the most from your central venous pressure catheter. ASA Refresher Courses Anesthesiol. 1995;23:157–75.
58. Mark JB. Central venous pressure monitoring: clinical insights beyond the numbers. J Cardiothorac Vasc Anesth. 1991;5(2):163–73.
59. Mark JB. Arrhythmias. Atlas of cardiovascular monitoring. New York: Churchill Livingstone; 1998. p. 219–45.
60. Mark JB. Patterns of valvular heart disease. Atlas of cardiovascular monitoring. New York: Churchill Livingstone; 1998. p. 286–312.
61. Snyder RW, Glamann DB, Lange RA, Willard JE, Landau C, Negus BH, et al. Predictive value of prominent pulmonary arterial wedge V waves in assessing the presence and severity of mitral regurgitation. Am J Cardiol. 1994;73(8):568–70.
62. Moore RA, Neary MJ, Gallagher JD, Clark DL. Determination of the pulmonary capillary wedge position in patients with giant left atrial V waves. J Cardiothorac Anesth. 1987;1(2):108–13.
63. Lorell B, Leinbach RC, Pohost GM, Gold HK, Dinsmore RE, Hutter AM, et al. Right ventricular infarction. Clinical diagnosis and differentiation from cardiac tamponade and pericardial constriction. Am J Cardiol. 1979;43(3):465–71.
64. Kushwaha SS, Fallon JT, Fuster V. Restrictive cardiomyopathy. N Engl J Med. 1997;336(4):267–76.
65. Kern MJ, Aguirre F. Interpretation of cardiac pathophysiology from pressure waveform analysis: pericardial compressive hemodynamics, Part I. Cathet Cardiovasc Diagn. 1992;25(4):336–42.
66. Mitchell J, Gilmore J, Sarnoff S. The transport function of the atrium. Factors influencing the relation between mean left atrial pressure and left ventricular end diastolic pressure. Am J Cardiol. 1962;9:237–47.
67. Gidwani UK, Mohanty B, Chatterjee K. The pulmonary artery catheter: a critical reappraisal. Cardiol Clin. 2013;31(4):545–65.

Journal of Clinical Monitoring and Computing
https://doi.org/10.1007/s10877-021-00673-5

REVIEW PAPER

# The contemporary pulmonary artery catheter. Part 2: measurements, limitations, and clinical applications

**I. T. Bootsma[1] · E. C. Boerma[1] · T. W. L. Scheeren[2] · F. de Lange[1]**

Received: 14 September 2020 / Accepted: 8 February 2021


## Abstract

Nowadays, the classical pulmonary artery catheter (PAC) has an almost 50-year-old history of its clinical use for hemodynamic monitoring. In recent years, the PAC evolved from a device that enabled intermittent cardiac output measurements in combination with static pressures to a monitoring tool that provides continuous data on cardiac output, oxygen supply and-demand balance, as well as right ventricular performance. In this review, which consists of two parts, we will introduce the difference between intermittent pulmonary artery thermodilution using bolus injections, and the contemporary PAC enabling continuous measurements by using a thermal filament which heats up the blood. In this second part, we will discuss in detail the measurements of the contemporary PAC, including continuous cardiac output measurement, right ventricular ejection fraction, end-diastolic volume index, and mixed venous oxygen saturation. Limitations of all of these measurements are highlighted as well. We conclude that thorough understanding of measurements obtained from the PAC is the first step in successful application of the PAC in daily clinical practice.

**Keywords** Hemodynamic monitoring · Pulmonary artery catheter · Thermodilution · Continuous cardiac output · Right ventricular ejection fraction · Right ventricular end-diastolic volume · Mixed venous oxygen saturation · Oxygen supply and -demand balance

## Abbreviations

| | |
|---|---|
| CO | Cardiac output |
| CCO | Continuous cardiac output |
| CCI | Continuous cardiac index |
| CVP | Central venous pressure |
| EDV | End-diastolic volume |
| EDVi | End-diastolic volume index |
| Hb | Hemoglobin |
| HFpEF | Heart failure with preserved ejection fraction |
| ICU | Intensive care unit |
| LV | Left ventricle |
| LVEDP | Left ventricular end-diastolic pressure |
| LVEDV | Left ventricular end-diastolic volume |
| MAP | Mean arterial pressure |
| MPAP | Mean pulmonary artery pressure |
| MRI | Magnetic resonance imaging |
| PA | Pulmonary artery |
| PAC | Pulmonary artery catheter |
| PAP | Pulmonary artery pressure |
| PAPi | Pulmonary artery pulsatility index |
| PAWP | Pulmonary artery wedge pressure |
| PEEP | Positive end-expiratory pressure |
| PH | Pulmonary hypertension |
| RV | Right ventricle |
| RVEDV | Right ventricular end-diastolic volume |
| RVEF | Right ventricular ejection fraction |
| $ScvO_2$ | Central venous oxygen saturation |
| $SvO_2$ | Mixed venous oxygen saturation |
| SV | Stroke volume |
| SVi | Stroke volume index |
| TR | Tricuspid regurgitation |
| $VO_2$ | Systemic oxygen consumption |

✉ I. T. Bootsma
ingebootsma@gmail.com

[1] Department of Intensive Care, Medical Center Leeuwarden, Henri Dunantweg 2, P.O. Box 888, 8901 Leeuwarden, the Netherlands

[2] Department of Anesthesiology, University of Groningen, University Medical Center Groningen, Groningen, the Netherlands

Published online: 01 March 2021

## 1 Introduction

Since the introduction of the original floating pulmonary artery catheter (PAC) by Swan and Ganz in 1970 the device has changed considerably. The classical PAC evolved from a catheter that enabled intermittent cardiac output (CO) measurements in combination with static pressures to a monitoring tool which provides continuous data on CO, the oxygen delivery and consumption balance, as well as right ventricular (RV) performance. Detailed understanding of the technology and its potential pitfalls are eminent in adequate interpretation of PAC-derived data. However, a large proportion of ICU physicians and critical care nurses in Europe and the United States failed to answer even the most basic questions concerning the PAC and its measurements [1, 2]. The aim of this narrative review is to provide an overview of the existing knowledge on the use of the contemporary PAC in critically ill and perioperative patients. This CCO-PAC, further mentioned as PAC, is a 7.5 F continuous cardiac output (CCO)/mixed venous oxygen saturation ($SvO_2$)/ end diastolic volume (EDV)-pulmonary artery catheter (model 774F75; Edwards Lifesciences, Irvine, CA, USA). In the first part of this review we discussed adequate placement, interpretation of waveforms, as well as pitfalls of this PAC. In this second part of the review, we highlight measurements of the additional information that comes from the technological innovations of the contemporary PAC, including the measurement of CCO, RV ejection fraction (RVEF), end-diastolic volume index (EDVi), and $SvO_2$. Limitations and clinical applications of these measurements are addressed in detail.

## 2 Measurements

Measurements obtained from the PAC can be found in Table 1. It is of note that for accurate measurements the PAC should be placed in the correct position within the

**Table 1** Hemodynamic variables obtained from the pulmonary artery catheter

| Variable | Abbreviation | Equation | Normal range |
|---|---|---|---|
| Mixed venous oxygen saturation | $SvO_2$ | n.a | 60–80% |
| Cardiac output | CO | HR × SV/1000 | 4.0–8.0 L $min^{-1}$ |
| Cardiac index | CI | CO/BSA | 2.5–4.0 L $min^{-1}$ $m^{-2}$ |
| Cardiac power index | CPI | (MAP-CVP) × CI/451 | 0.5–0.7 W $m^{-2}$, population specific |
| Central venous Pressure | CVP | n.a | 2–6 mmHg |
| Stroke volume | SV | CO/HR × 1000 | 60–100 mL |
| Stroke volume Index | SVi | CI/HR × 1000 | 33–47 mL $m^{-2}$ |
| Stroke volume variation | SVV | (SVmax-SVmin)/SVmean × 100 | 10–15% |
| Systemic vascular resistance | SVR | 80 × (MAP − CVP)/CO | 800–1200 dynes sec $cm^{-5}$ |
| Systemic to pulmonary pressure ratio | MAP/MPAP | MAP / MPAP | 4.0 ± 1.4 in uncomplicated cardiac surgey |
| Pulmonary artery systolic pressure | PASP | n.a | 15–30 mmHg |
| Pulmonary artery diastolic pressure | PADP | n.a | 8–15 mmHg |
| Pulmonary artery wedge pressue | PAWP | n.a | 6–12 mmHg |
| Pulmonary vascular resistance | PVR | 80 × (MPAP − PAWP)/CO | < 250 dynes sec $cm^{-5}$ |
| Pulmonary artery pulsatility index | PAPI | (PASP − PADP)/CVP | population specific |
| LV stroke work index | LVSWi | SVi × (MAP − PAWP) × 0.0136 | 50–62 mmHg ml $m^{-2}$ |
| RV stroke work index | RVSWi | SVi × (MPAP − CVP) × 0.0136 | 5–10 mmHg ml $m^{-2}$ |
| RV function index | RFI | PASP/CI | 31.7 ± 16.7 in ICU survivors with PH |
| RV end-diastolic volume | RVEDV | SV/EF | 100–160 mL |
| RV end-diastolic volume index | RVEDVi | RVEDV/BSA | 60–100 mL $m^{-2}$ |
| RV end-systolic volume | RVESV | EDV-SV | 50–100 mL |
| RV ejection fraction | RVEF | (SV/EDV) × 100 | 40–60% |
| RV systolic pressure | RVSP | n.a | 15–30 mmHg |
| RV diastolic pressure | RVDP | n.a | 2–8 mmHg |

*BSA* body suface area; *CI* cardiac index; *EDV* end diastolic volume; *EF* ejection fraction; *HR* heart rate; *LV* left ventricle; *MAP* mean arterial pressure; *MPAP* mean pulmonary arterial pressure; *n.a.* not applicable; *PAWP* pulmonary artery wedge pressure; *PH* pulmonary hypertension; *RV* right ventricle

Adapted from: Edwards Clinicical Education Quick Guide to Cardiopulmonary Care [4]

pulmonary artery. This procedure is described in detail in the first part of this review [3].

## 3 Cardiac output

### 3.1 Intermittent cardiac output measurements

The Fick method is the gold standard for indirect CO determinations. This method determines the cardiac output as the quotient of systemic oxygen consumption ($VO_2$) and the difference between arterial and mixed venous oxygen content.

The oxygen concentration in arterial blood is a function of the hemoglobin concentration (Hb) and the percent saturation of hemoglobin with oxygen ($SaO_2$). The CO can then be calculated using the following formula:

$$-CO\,(mL\,\mathrm{min})^{-1} = \frac{VO_2}{1.34xHbx\left(SaO_2 - SvO_2\right)}$$

In this formula, $VO_2$ (in mL $\mathrm{min}^{-1}$) = oxygen consumption as directly measured by respirometry [5], $SvO_2$ (in %) is the mixed venous oxygen saturation. Since this direct Fick technique is technically demanding at the bedside, it is rarely used in clinical practice.

Intermittent pulmonary artery thermodilution is the clinical reference method for CO measurement [6]. To measure CO using pulmonary thermodilution, a bolus of cold crystalloid solution is injected in the central venous circulation. The cold indicator bolus injection causes a decrease in blood temperature that is detected downstream using a thermistor near the catheter tip. From the thermodilution curve, which represents the changes in blood temperature over time, CO can be calculated using a modified Stewart-Hamilton formula:

$$CO = \frac{Vx(Tb - Ti)}{A} x \frac{SIxCI}{(SBxCB)} x \frac{60xCTxK}{1}$$

In this formula, CO = cardiac output, V = volume of injectate, A = area of thermodilution curve in square mm divided by paper speed (mm/sec), K = calibration constant in mm/°C, Tb = temperature of blood, Ti = temperature of injectate, SB = specific gravity of blood, SI = specific gravity of injectate, CB = specific heat of blood, CI specific heat of injectate,

$$\frac{SIxCI}{(SBxCB)} = 1.08$$

when 5% dextrose is used, CT is correction factor for injectate warming.

Intermittent pulmonary artery thermodilution with cold-saline bolus injections has multiple limitations. The modified Steward-Hamilton equation shows that the bolus-derived information depends on injected volume, rate, and temperature. Overestimation of CO can occur in the presence of left-to-right or right-to-left intracardiac shunts, the use of a small injection volume, or a higher injectate temperature as compared to the reference temperature. All of these causes result in a smaller area under the thermodilution curve, resulting in an overestimated CO. Tricuspid regurgitation (TR) might both under- and overestimate CO due to increased transit time and modified blood temperature in the right atrium. Pulmonary valve insufficiency changes the appearance of the thermodilution curve, but CO measurement generally remains accurate since the area under the thermodilution curve is not affected, unless the CO is very low [7]. Underestimation of CO is mainly seen in high-flow states due to rapid temperature changes in the pulmonary artery [8–11]. In addition, inadequate timing during the respiratory cycle and variability in injection technique may further influence the accuracy of bolus thermodilution CO measurements [12]. Bolus CO measurements are therefore highly user-dependent [13]. Over the years a continuous measurement system has been developed in order to overcome these disadvantages. In the early days, placement of a heating filament was severely compromised due to background thermal noise in the pulmonary artery or because of limitations either in maximum peak heat flux or in temperatures [14, 15]. To overcome these limitations, a combination of thermal indicator dilution and a stochastic system is now used in the modern PAC. To this end, the contemporary PAC is equipped with a 10 cm long thermal filament, positioned 15–25 cm from the tip of the catheter. This filament heats up the blood in a random on–off pattern. The change in blood temperature is measured downstream by the thermistor throughout the entire respiratory cycle. Based on a repeating on–off signal, a relaxation waveform can be generated. This technique enables measurement of true volumetric flow and is independent of the physical geometry of the system. Detailed information about the used algorithm and the stochastic system has been described previously [16].

### 3.2 Continuous cardiac output measurement

Using the area under the relaxation thermodilution waveform, near-continuous and almost real-time measurement of CCO can be obtained. CCO measurement with PAC is well-validated in experimental settings nowadays, as well as in different patient categories [17–20]. CCO was shown to be more accurate when compared to various other measurement methods for CO, including electromagnetic measurement of aortic blood flow, bolus thermodilution, the Fick method, and aortic transit-time ultrasound [18, 21–25]. In addition, CCO showed to be more accurate and less variable when compared to the intermittent bolus thermodilution

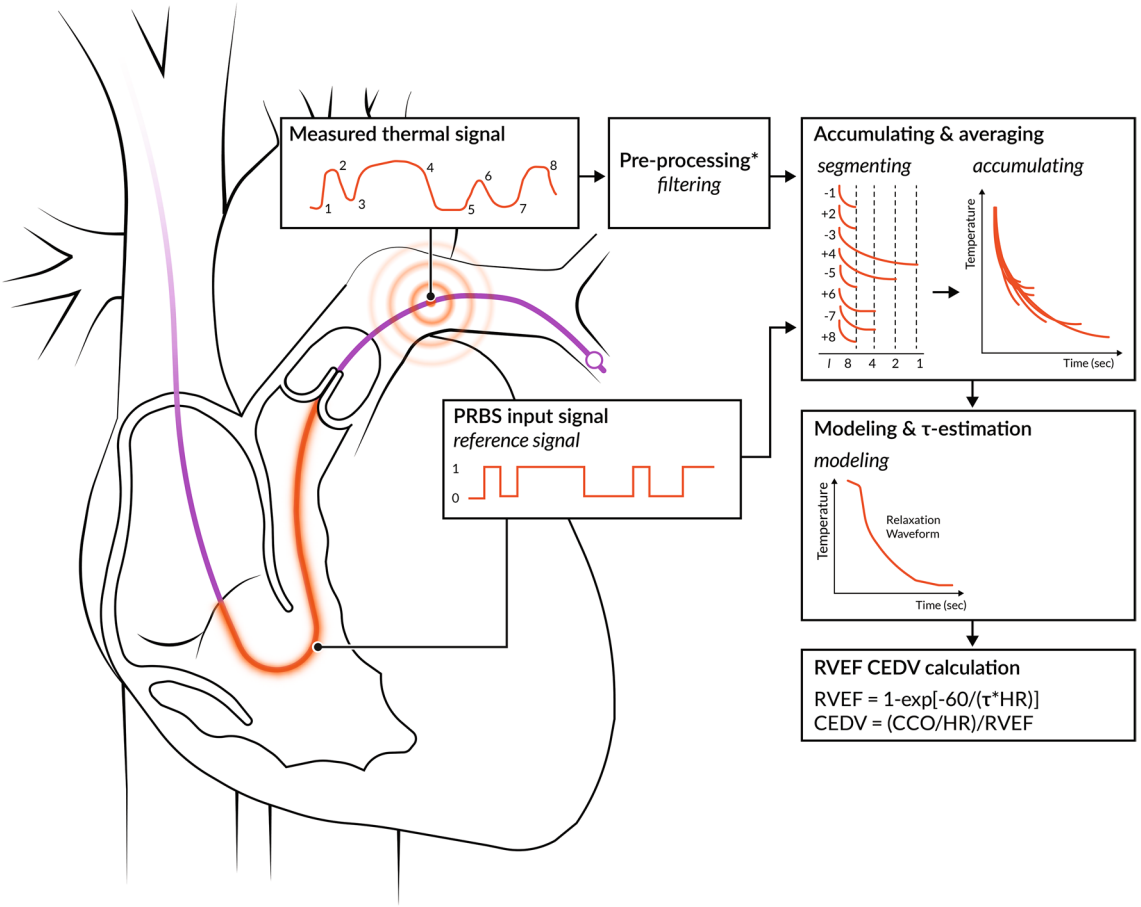


**Fig. 1** Relaxation waveform for continuous cardiac output and concomitant calculations of right ventricular ejection fraction and right ventricular end-diastolic volume calculations. Shown are the thermal signal sent out by the proximal part of the PAC, how this is received in the more distal part of the PAC, and how this is transformed to derive the specific variables. PRBS Pseudo-Random Binary Sequence; RVEF right ventricular ejection fraction. CEDV continuous right ventricular end-diastolic volume. CCO continuous cardiac output. τ = exponential decay time constant. * This step is skipped when using STAT-CCO over trend CCO monitoring. Adapted from: Wiesenack C et al. [46]

technique. The CCO method is independent of the clinician, injection technique, and injection volume. Furthermore, the CCO method is not influenced by ventilator settings due to a high sampling rate at random time points in the ventilatory cycle (Fig. 1). This allows for detection of smaller variations in CO, as well as good performance over a wide range of CO and blood temperatures [24, 26].

## 4 Limitations of cardiac output measurements

### 4.1 Delayed response in CCO measurement results

It is important to distinguish two different ways of depicting CCO measurement results: trend CCO and STAT CCO. The trend CCO reflects the average CCO over the previous 4–12 min (depending on the monitor setting) [27, 28]. During rapid alterations of hemodynamic state there is a clinically important time lag in the response of the trend CCO [28]. The STAT CCO was designed to improve the response time. Using a faster algorithm, STAT CCO is updated every 30–60 s and has shown good accuracy and precision compared to intermittent pulmonary artery thermodilution [28]. Pacing-induced hemodynamic changes, for instance, were detected in mean arterial pressure (MAP) recordings after 30 s, and an increase in $SvO_2$ reached significance after 90 s. A significant increase in CCO using the STAT algorithm was reached after a minimum of 270 s [28]. Physicians should be aware of a delayed response, even when using the STAT mode [29, 30], limiting the use of this method in dynamic hemodynamic assessments (e.g. of fluid responsiveness).

### 4.2 Intracardiac shunts

In vitro experiments have shown that shunting 50% of total blood flow results in mean systematic errors of − 26.8 (± 8.2%) for CCO measurements during an intracardiac left-to-right shunt, overestimating true values as a result of altered waveform configuration [24]. Although the CO is falsely high in the setting of intracardiac shunts, the PAC may be useful in both detecting the presence and assessing the magnitude of the intracardiac left-to-right shunt.

### 4.3 Tricuspid regurgitation and tachycardia

TR has been associated with an underestimation or overestimation of CO, and even with no influence on CO measurements [31, 32]. In general, a high degree of TR is associated with an underestimation of true CO [33]. In patients with pulmonary hypertension, the agreement between the Fick method and thermodilution CO was not affected by the severity of TR [34]. However, despite possible under- or overestimation of CCO in the presence of TR, CCO measurements remain clinically relevant when using this method for trend monitoring, as well as to assess the response to hemodynamic interventions [35]. Furthermore, when using the CCO method, it might be expected that the influence of TR is less pronounced when compared with the intermittent bolus CO technique, because CCO represents an average value over time and is less dependent on interindividual variations in infusion. However, firm data on this remain scarce [26].

### 4.4 Fluid administration

The infusion of fluid through the side-ports of the sheath, or through the venous port of the PAC, influences the thermodilution washout curve. During bolus thermodilution measurements this leads to an artefactual increase in the area under the curve, and thus to an underestimation of CO [36, 37]. Although it is suggested that the continuous measurement system is less accurate during fluid infusion [38], various infusion rates of lactated Ringer's solution (100, 200, 500, 1000 ml $h^{-1}$) only influenced the CCO values at a low-flow rate equal to or below 2 L $min^{-1}$. In contrast, intermittent bolus CO measurements were affected at all flow rates. Thus, CCO measurements seem to have a better resistance to the thermal noise produced by high rates of infusions as compared to the bolus method [24].

### 4.5 Extreme temperature variations

Extreme temperature variations can cause a poor correlation between intermittent bolus CO measurements and CCO measurements. In patients treated with therapeutic hypothermia after cardiac arrest, for instance, a low correlation coefficient was observed with broad limits of agreement when comparing thermodilution CCO with indirect Fick CO measurements [39]. Conflicting results were found in small, non-randomized trials in the setting of post cardiopulmonary bypass [40, 41]. In patients undergoing orthotopic liver transplantation, both CCO and bolus CO methods showed decreased accuracy and precision after caval clamping and reperfusion [20]. However, since the accuracy of bolus CO among hypothermic patients is a topic of debate, this method may not necessarily be considered the standard for comparison in this specific setting. It is of note that in vitro measurements indicate that the CCO technique has a greater resistance to thermal noise compared to bolus CO measurements providing a higher accuracy [24].

## 5 Right ventricular ejection fraction and end-diastolic volume

At the end of the 1980′s, a PAC enabling measurement of both RVEF and right ventricular end-diastolic volume (RVEDV) was introduced. This PAC was validated against various other RVEF measurements methods, including angiography, contrast ventriculography, and echocardiography [42–44]. Nowadays, the PAC enables continuous measurement of the RVEF and RVEDV by using the exponential decay time constant (τ) of the thermodilution relaxation waveform, combined with the heart rate (HR) (Fig. 1). RVEF is calculated as follows:

$$RVEF = 1 - \exp\frac{-60}{\tau xHr} \; or \; RVEF = 1 - \frac{Tb2 - Tb0}{Tb1 - Tb0}$$

where Tb0 = blood temperature before heat application, Tb1 = blood temperature during the first subsequent systole, and Tb2 = blood temperature during the successive systole [45]. Once RVEF is obtained, calculations of RVEDV are based on CCO, HR, and RVEF using the following calculation [46]:

$$RVEDV = \frac{(CCO/HR)}{RVEF}.$$

Because RVEDV is derived from RVEF and CO, errors in RVEDV are a combination of errors in both CO and RVEF measurements. Nevertheless, RVEDV has been proven to be highly predictive for volumes in a pulsatile flow model [47]. Measurements of RVEF and RVEDV are neither dependent on bolus volume nor on the temperature

of the injected fluid. Moreover, in CCO, the PAC filaments heat up the blood directly in the RV, bypassing the influential effects of the right atrium, leaving the conservation of energy and RV dynamics and RV afterload as the primary determinants of the thermal washout curve [48]. As a result, previous studies using the bolus thermodilution technique may not directly be comparable with the CCO approach using the heating filament. Although the continuous thermodilution technique is currently validated for CCO measurements, there is lack of data concerning validation of RVEF and RVEDV. Overall, both reproducibility and accuracy of the continuous method are superior compared to the intermittent bolus technique [24, 26]. Since the RVEF uses the washout thermodilution curve, all factors that confound CO measurements will also interfere with an accurate determination of RVEF.

### 5.1 Limitations of the continuous RVEF measurements: Underestimation

In general, every measurement method has its own unique reference values. Thermodilution-derived RVEF seems to underestimate RVEF when compared to other measurement methods such as ultrasound, magnetic resonance imaging (MRI), and radionuclide angiography [42, 43, 45, 49–51]. Animal research revealed that this underestimation was most likely explained by the fact that the blood in the right atrium did not return to baseline temperature within a single heartbeat after the cold fluid injection [48]. Although thermodilution with the continuous measurement technique takes place in the RV instead of the right atrium, the continuous RVEF still seems to be underestimated by the PAC [45]. New 4D MRI technology has revealed that the blood temperature did not return to baseline within a single heartbeat as a result of the phasic contraction pattern of the RV. For every systolic beat, only 44% of the EDV contributed directly to the pulmonary artery flow [52]. Recirculation of blood in the RV might result in it taking more time for the heat mass to reach the thermistor. As a consequence of the prolonged relaxation, waveform RVEF will be underestimated and RVEDV will be overestimated. Whether or not the absolute volume data is completely correct does not influence whether these measurements are precise, and the fact remains that they can be of great value for trend monitoring. In general, an absolute correction factor of + 11% will result in a more realistic absolute value of RVEF [48].

### 5.2 Mathematical coupling

Since the formula of RVEDV contains the CO by dividing stroke volume (SV) by RVEF, the correlation between those two variables may be explained by mathematical coupling. However, various studies examining the relationship between RVEDV and CCO showed that this relationship remained significant even after statistical correction for potential mathematical coupling or by including an independent technique for CO measurements. Therefore, mathematical coupling alone does not explain the correlation between RVEDV and CO [53–55].

## 6 Mixed venous oxygen saturation

Mixed venous oxygen saturation ($SvO_2$) can be measured periodically in blood samples drawn from the distal lumen of the PAC in order to validate the measured values. Adding reflective fibreoptic oximetry at the distal end of the PAC enabled the clinician to accurately measure the $SvO_2$ on a continuous base [56]. Oximetry is based on the technique known as spectrophotometry. The absorption of specific wavelengths of light, as it passes through a medium, is proportional to the concentration of the substance that absorbs both the light waves and the travel length. Oxygenated Hb does not absorb red light waves (wavelength 660 nm) as well as deoxygenated Hb does. On the contrary, infrared light waves (wavelength 940 nm) are better absorbed by oxygenated Hb. The determinants of $SvO_2$ are identified in the following equation:

$$SvO_2 = SaO_2 - (VO_2CO \times 1.34 \times [HB]),$$

where $SaO_2$ is arterial oxygen saturation and $VO_2$ is systemic oxygen consumption. As such, $SvO_2$ reflects the balance between oxygen delivery ($DO_2$) and oxygen consumption ($VO_2$). A change in $SvO_2$ indicates an imbalance between oxygen delivery and consumption. However, further information is needed to assess the cause of this change. Therefore, $SvO_2$ is not a simplified index of inadequate CO, since there are more determinants in the formula. Alterations in $SvO_2$ might be due to changes in oxygen transport (arterial $SaO_2$, Hb, CO) or a change in body $VO_2$ [5].

## 7 Clinical application of PAC-derived data

### 7.1 Assessing fluid responsiveness

Over the years it has become clear that static filling pressures (CVP and PAWP) and cardiac preload should not be used interchangeably [57–59]. The pressure–volume relationship of the RV has a triangular shape, due to the low pressure and high capacitance characteristics of the pulmonary vascular bed. The RV pressure–volume relationship changes with different loading conditions, which can result in an increased filling pressure associated with a decreased filling volume [60, 61]. A change in preload does not result in a

proportional change in filling pressures [62]. Although CVP and PAWP are not suitable for preload assessment, this does not mean that they should not be measured at all. An important determinant of organ perfusion pressure is the difference between the inflow pressure (MAP) and the outflow pressure (CVP). Both lower MAP and elevated CVP can result in diminished organ perfusion. Among different patient categories, an association between elevated CVP and impaired microcirculatory blood flow or increased risk of acute kidney and liver injury has been demonstrated [63–65]. Elevated or rapidly rising values of CVP and PAWP may serve as a stop rule for fluid resuscitation [66]. An increase in CVP in response to a fluid challenge without a change in CO is an indicator for poor fluid responsiveness and should alert the clinician of a possible RV dysfunction [66, 67]. The work of Guyton showed how venous return curves interact with cardiac function curves, i.e. right atrial pressure not being the primary determinant of CO rather than itself being determined by CO [68, 69]. When combining this knowledge with blood pressure difference (MAP-CVP) and CO, clinicians are offered a potential approach regarding the application of CVP in the clinical setting (Table 2) [70]. Although it has been shown that many intensive care physicians do not measure CO, it is highly recommended when trying to obtain a better understanding of both the hemodynamic situation and the effects of goal-directed management [71].

Today, static filling pressures are replaced by the concept of fluid responsiveness. The Frank-Starling curve depicts SV on the vertical axis and cardiac preload on the horizontal axis. On the steep part of the curve, an increase in preload will result in a significant increase in SV. At higher values of cardiac filling pressures, the curve flattens and an increase

**Table 2** PAC-derived variables in the clinical setting

| Clinical situation | PAC derived variables | Clinical interpretation |
|---|---|---|
| Low arterial blood pressure | ↓ CCI + ↑ CVP | Decrease in venous return, e.g. reduced cardiac function or hypovolemia |
| | ↑ CCI + ↓ CVP | Increase in venous return, e.g. distributive shock |
| Fluid responsiveness | ↑ SV or CCI ≥ 15% after 250 ml or 3 ml $kg^{-1}$ of crystalloid | Patient will probably benefit from fluid administration |
| RV dysfunction and failure | Early stage (moderate RV dysfunction = RVEF 20–30%):<br>↓ RVEF, ↑ EDVi, CCI = N,<br>$SvO_2$ = N<br>CVP N or ↑ | |
| | Advanced stage (severe RV dysfunction = RVEF < 20%):<br>↓↓ RVEF, ↑ EDVi, ↓ CCI,<br>↓ $SvO_2$, ↑ CVP | |
| LV failure | ↑ PAP, ↑ PAWP, ↓ CCI | |
| Intracardiac shunt | ↑↑ $SvO_2$ | ≥ 6% step up $ScvO_2$ to $SvO_2$ indicates a L-R shunt |
| Weaning- from-ventilator | ↑ PAWP, ↓ $SvO_2$ during weaning trial | Weaning-induced cardiac failure |
| Pulmonary hypertension | Pre-capillary:<br>PAWP = N<br>Post-capillary:<br>↑ PAWP (> 15 mmHg) | Echocardiographic assesment should rule out HFpEF |
| Tamponade post cardiac surgery* | ↓ CCI, ↑/ = CVP, ↓ $SvO_2$,<br>↓ EDVi, ↓ RVEF, ↑ PAWP | Compression of the RV free wall causes low RVEDV despite substantial fluid administration |
| Distributive shock | ↑ CCI, ↑ $SvO_2$, ↓/ = CVP, ↓/ = PAWP | Septic, neurogenic, anaphylactic, toxin-induced, or endocrine shock |
| Hypovolemic shock | ↓ CCI, ↓ $SvO_2$, ↓CVP,<br>↓ PAWP | Hemorrhagic, gastrointestinal, skin, renal, or third space fluid losses |
| Cardiogenic shock | ↓ CCI, ↓ $SvO_2$, ↑/ = CVP,<br>↑ PAWP | Cardiomyopathic, arrhythmic, or mechanical causes |
| Obstructive shock | ↓ CCI, ↓ $SvO_2$, ↑ CVP,<br>↑ PAWP | PH, pulmonary embolism, tension pneumothorax, tamponade, pericarditis, restrictive cardiomyopathy |

*The location of the bleeding/hematoma determines the hemodynamic profile of the patient

*N* normal; *CCI* continuous cardiac index; *CVP* central venous pressure; *SV* stroke volume; *RV* right ventricle; *RVEF* right ventricular ejection fraction; *EDVi* end-diastolic volume index; *$SvO_2$* mixed venous oxygen saturation; *$ScvO_2$* central venous oxygen saturation; *PAP* pulmonary artery pressure; *PAWP* pulmonary artery wedge pressure; *LV* left ventricle; *HFpEF* heart failure with preserved ejection fraction; *PH* pulmonary hypertension; *HFpEF* heart failure with preserved ejection fraction

in preload will not result in an increase in SV [72]. In this respect there are three relevant questions in the clinical setting: (1) At which part of the Frank-Starling curve does the heart of the patient operate? (2) Is the patient fluid responsive? (3) Are fluids beneficial? Irrespective of the answers to question 1 and 2, the clinician does need to determine whether fluids are beneficial to the patient, or whether another therapeutic approach is needed or better suited to the situation, since being fluid responsive is not equivalent to being in need for fluids. Fluid challenges should be performed with 250 ml or 3 ml $kg^{-1}$ crystalloid, which is infused over a short period of time (5–10 min). Fluid responsiveness is most often defined as an increase $\geq 15\%$ in stroke volume index (SVi) or cardiac index (CI) after a fluid challenge (Table 2) [73]. SVi or CI should be the primary target, and neither arterial blood pressure nor ventricular filling pressures or volumes should be used as a surrogate for fluid responsiveness [74]. CI and SVi measured with the PAC are highly predictive of actual pulsatile flow [47]. Since the PAC is able to measure both fluid responsiveness variables (SVi and CI) and target/safety thresholds (CVP and PAWP) in a continuous manner, it can be used to manage fluid therapy adequately [29, 30]. In addition, a rise in RVEDP during fluid administration, in the absence of a change in CO, is indicative for RV volume overloading and a reason for the clinician to stop the intervention.

### 7.2 Right ventricular dysfunction and failure

Acute RV dysfunction can occur due to a variety of diseases, resulting in an increase in RV afterload, decreased contractility, or an increase/decrease in RV preload. A decreased RV function can induce a vicious circle of RV failure. When having a closer look at hemodynamics during RV failure, ventricular interdependence is an important concept to keep in mind. Due to shared muscle fibers, septal wall, and pericardium, mechanical forces can be transmitted from one ventricle to the other, both in systole and diastole [75]. RV volume/pressure overload or diminished contractility will result in RV dilatation. The intraventricular septum will flatten during diastole in case of volume overload and mainly during systole in case of pressure overload, creating a D-shaped LV [75, 76]. RV diastolic dysfunction and RV dilatation will shift the pressure–volume curve of the LV towards higher pressures, due to decreased LV diastolic compliance [75]. Furthermore, increased LV end-diastolic pressure (LVEDP), reduced LV transmural filling pressure, and impaired LV diastolic filling as a result of the septal shift will contribute to low CO and ultimately to low blood pressure [77]. In severe RV failure, low blood pressure in combination with high RV filling pressures result in severely reduced organ perfusion, due to a reduced difference between MAP and CVP, being an important determinant of the driving force for venous return [78]. It is of note that a normal CO, or normal pulmonary artery pressure (PAP), does not exclude RV dysfunction [79, 80]. Classically, the diagnosis of RV failure is made by combination of clinical assessment (i.e. signs of impaired organ perfusion in combination with venous congestion) and echocardiographic evaluation. To classify RV failure, a number of reference values for a variety of echocardiographic measures have been suggested [81]. Providing RV volume and pressures with the PAC, as well as contractility measurements, can be helpful in diagnosing and managing RV failure. In Table 1 reference values for RVEF and RVEDV have been provided, as stated by the manufacturer. However, it is pivotal to understand that reference values for PAC-derived RVEF in the clinical setting may be considerably lower, also in comparison to 2D or 3D echocardiography. Based on datasets, combining RVEF with long-term outcome in cardiac surgery and sepsis, we suggest the following classification: RVEF < 20%: severe RV dysfunction; RVEF 20–30%: moderate RV dysfunction: RVEF > 30%: no RV dysfunction [82, 83]. Under physiological conditions, an increase in RVEDV is compensated by an (immediate) increase in SV, referred to as heterometric autoregulation [84]. However, in the early stage of RV dysfunction, RV dilatation becomes an adaptive mechanism for the preservation of adequate preload, reflected by a higher EDV and lower RVEF. When RV failure is combined with, or secondary to, LV failure, PAWP can be elevated (Table 2). In a more progressive disease state, CO will be diminished as well. The CVP waveform can reveal a prominent v-wave due to TR in response to RV dilatation [85].

Nowadays, new hemodynamic indices, derived from PAC measurements, might be helpful in early identification of RV dysfunction. The pulmonary artery pulsatility index (PAPi) is defined as: (systolic PAP − diastolic PAP) / CVP. This index predicts severe RV failure and has additive value in the setting of advanced heart failure, cardiogenic shock, and left ventricular assist device therapy. However, PAPi measurements and thresholds vary significantly between studies of different patient populations and thresholds from one patient population should not be extrapolated to another patient group [86].

Another index is the ratio of pulmonary artery effective elastance ($E_a$) to RV maximal end-systolic elastance ($E_{max}$). This right ventriculo-arterial coupling index relates to the mechanical efficiency of the RV, and is ideally derived from RV pressure–volume loops. Nowadays, bedside estimation can be obtained by this ratio, using the contemporary PAC. $E_a$ and $E_{max}$ can be defined as $E_a$ = mean PAP

$$\mathrm{MPAP} - \mathrm{PAWP}/\mathrm{SV},$$

and $E_{max} = \mathrm{MPAP}/\mathrm{RVEDV} - \mathrm{SV}$.

The ratio $E_a/E_{max}$ equals 1 in case of optimal ventricular-vascular coupling. Hence, $E_a/E_{max}$ may help in early identification of RV dysfunction in critically ill patients [87].

Under conditions of impaired RV function, analysis of the RV waveform can be useful in early detection and subsequent management of RV dysfunction, especially during cardiac surgery [88–90]. Since RV pressure monitoring requires a different PAC with a dedicated RV pace-port, further details are beyond the scope of this review.

### 7.3 Left heart failure

To distinguish isolated RV failure from a combination of RV and LV failure, the use of PAC may be helpful. Of note, LV filling pressures cannot be reliably estimated by means of clinical examination [91]. Classically, in case of combined LV and RV failure, CI and $SvO_2$ are low, and PAWP is elevated [92]. In patients with a PAWP ≥ 15 mmHg, LV failure is likely [93]. In case of a low or normal PAWP, isolated RV failure is more likely. However, a PAWP ≤ 15 mmHg does not rule out the presence of LV failure, in particular in patients with LV heart failure and preserved ejection fraction (HFpEF) [94]. In this case, further echocardiographic evaluation of diastolic LV function is recommended (Table 2).

### 7.4 The detection of left-to-right shunts

A high $SvO_2 > 75\%$ may indicate a cardiac left-to-right shunt. For oximetric shunt detection, blood sampling from the distal channel in the PAC and the proximal channel in the vena cava superior or right atrium is needed. Under physiological conditions, oxygen saturation in the pulmonary artery is lower than that in a central vein, due to the contribution of desaturated blood flow from the coronary sinus. However, when a left-to-right shunt is present, oxygenated blood can cause an increase in oxygen saturation at the tip of the PAC. A step up of > 6% in oxygen saturation from the vena cava superior to the pulmonary artery is suggestive of the presence of a left-to-right shunt (Table 2) [95]. Using the $SvO_2$ and the central venous saturation ($ScvO_2$) in combination with the arterial oxygen saturation ($SaO_2$), a shunt fraction can be calculated according to the following equation:

$$Qp/Qs = (SaO_2 - (SvO/SpvO_2)/(SpvO_2 - SpaO_2),$$

where Qp = pulmonary blood flow, Qs = systemic blood flow, $SaO_2$ = arterial oxygen saturation, $SvO_2$ = central venous oxygen saturation, $SpvO_2$ = pulmonary vein oxygen saturation (in the absence of a right to left shunt, this is identical to $SaO_2$), and $SpaO_2$ = pulmonary artery oxygen saturation [95].

### 7.5 Ventilator weaning-induced cardiac failure

When switching from positive pressure ventilation (with and without positive end-expiratory pressure; PEEP) to spontaneous breathing, intrathoracic pressure falls during both inspiration and expiration compared to assisted ventilation. In response, right atrial pressure falls and venous return increases, resulting in an increase in RV preload, an increase in CO (in the fluid responsive patient), and in LV preload. In addition, the negative intrathoracic pressure results in an increase in LV afterload [96]. Besides these pressure changes, hypoxemia, hypercapnia, and an increased sympathetic tone can result in an increase of RV or LV afterload. However, in a specific subgroup of patients, right atrial pressure may rise during a spontaneous breathing trial [97]. This might be explained by an increase in intrinsic PEEP due to expiratory muscle activity or dynamic hyperinflation [98, 99]. When following this line of thought regarding physiology, one can see that an elevated PAWP can be the result of an increase in LV preload in patients with an already elevated LV end diastolic volume (LVEDV), an increase in afterload, for example due to a subsequent increase in mitral insufficiency, or a decrease in LV compliance (or a combination of these). In a landmark paper [100], elevated PAWP (> 18 mmHg) during a spontaneous breathing trial was shown to be associated with subsequent weaning failure in patients diagnosed with severe chronic obstructive pulmonary disease. After restarting mechanical ventilation, all patients received diuretics, and the PAWP decreased markedly as compared to before treatment (9 vs. 25 mmHg). In addition, failure to wean the patient from the ventilator was also accompanied by a decrease in PAC-derived $SvO_2$ measurements, whereas $SvO_2$ remained unchanged in the successfully weaned patients. The same study revealed no change in CI combined with an elevation of PAP and PAWP, indicating an increase in both LV and RV afterload [101]. PAC measurements can reveal weaning-induced cardiac failure, showing the response of the RV and LV during spontaneous breathing, as well as providing information about the change in the $VO_2/DO_2$ balance during this critical period. In daily practice, PAWP should be measured before and after a 30 min spontaneous breathing trial [102]. A T-piece weaning trial challenges patients' efforts and the LV performance the most. Other ways of conducting weaning trials, such as applying low levels of pressure support ventilation, might not reveal an elevation in PAWP (Table 2) [103].

### 7.6 Pulmonary hypertension

Right heart catheterization is the diagnostic gold standard for assessing pulmonary hypertension (PH), which was classically defined as a MPAP ≥ 25 mmHg at rest, and recently updated to a MPAP > 20 mmHg at rest [104–106]. In patients

with high MPAP, PAWP ≤ 15 mmHg is used to distinguish pre-capillary PH from high PAP pressures due to LV failure, since higher wedge pressures are related to left heart disease (Table 2) [93]. However, PAWP ≤ 15 mmHg does not rule out the presence of left heart failure, in particular in patients with HFpEF [94]. Relying on a single measurement can falsely label patients with an inaccurate diagnosis. In order to distinguish precapillary PH from HFpEF, additional echocardiographic assessment in combination with the assessment of risk factors associated with HFpEF may avoid misclassification [104]. Once the suspicion of PH has risen because of high PAP measurements, it is recommended to refer patients to an expert PH centre for further diagnosis and treatment early in the diagnostic process [107]. In the ICU, PH is rarely the primary cause of admission so that clinicians should search for underlying disease states that cause PH; however, exact data remain scarce [108]. Upon hospital admission, high PAP values are mostly seen as secondary to acute conditions, such as pulmonary embolism, acute respiratory distress syndrome, LV failure, or mitral valve regurgitation [109]. The classification of chronic PH is not always applicable in critical care settings and a different classification according to the underlying cause has been suggested [110]. Since the RV is not resistant to acute increases in afterload, acute PH can result in RV failure [111, 112].

### 7.7 Restrictive pathophysiology and tamponade

Pericardial constriction, restrictive cardiomyopathy, and RV infarction share the same underlying pathophysiologic feature; reduced RV diastolic compliance due to an increase in RV stiffness or impaired RV relaxation [113]. CVP waveform analysis can provide additional diagnostic clues for these conditions. Cardiac tamponade can be distinguished by the attenuation or disappearance of the y-descent in the CVP waveform. Obstructive shock due to tamponade results in a low CO, low SV, low MAP, and high CVP and RV filling pressures. Pulsus paradoxus can be present. In the final stage, there will be an equilibration of all cardiac and pulmonary artery diastolic pressures, which will result in an absence of coronary flow. This will finally lead to a circulatory arrest (Table 2) [114].

However, in the setting of postoperative cardiac surgery, the above described classical forms of waveforms and hemodynamic patterns may not be present during tamponade. The specific location of well-defined hematomas, rather than free mobile accumulation of fluid, determines the specific combination of alterations in waveforms, pressures, and volumes. For example, compression of the RV free wall by a localized hematoma may cause low RVEDV and low continuous cardiac index (CCI), despite substantial fluid administration, in combination with elevated or normal CVP (Table 2).

### 7.8 Determination of shock type

In shock, there is a mismatch between systemic oxygen delivery and oxygen demand. There are four types of shock; hypovolemic, cardiogenic, obstructive, or distributive. The PAC can be useful in identifying the type of shock, and it can be beneficial during the assessment of the hemodynamic status, as a prerequisite to select the adequate therapeutic intervention, and to evaluate the response to therapy. In current guidelines, if clinical examination alone does not lead to a diagnosis, use of the PAC is recommended in complex patients for the determination of the type of shock, in patients with refractory shock, and for shock in combination with RV dysfunction or acute respiratory distress syndrome [74, 115].

### 7.9 An integrative approach

Combining various variables may help to further elucidate the underlying mechanisms of RV failure, and strives beyond the strict interpretation of references values. For example, at first glance PAP values may not seem too far above the threshold for PH. But in case systemic blood pressure is below normal at the same time, such value may gain additional importance. The systemic to pulmonary pressure ratio (MAP/MPAP) is a tool to quantify such 'relative' PH and appeared useful in the prediction of hemodynamic complications during and after cardiac surgery [116]. Adjusting the PAP for a specific CI helps to quantify the RV workload, which is needed to maintain RV performance in the presence of a given afterload. The RV function index (RFI), defined as the systolic PAP(SPAP)/CI ratio, may be helpful to assess the additional amount of effort for the RV in case the flow or the afterload increases, and has predictive value as an independent risk factor for mortality in ICU patients with PH [117]. Finally, integrating the driving pressure (MAP-CVP) with the flow (CI), by means of a cardiac power output (CPO), elegantly acknowledges the fact that maintenance of the CI within the normal range, at the expense of an elevated CVP is less energy effective than maintaining an equal CI in the presence of a normal CVP [118]. As such, the CPO may be helpful to guide hemodynamic therapy into an acceptable range of MAP and CI, at the lowest possible level of $VO_2$.

## 8 Complications of the PAC

The invasive nature of the PAC implies the risk of complications. First of all, central venous access can result in accidental arterial puncture, air embolism, and pneumothorax. However, using ultrasound guidance during placement has been demonstrated to reduce the risk of catheter misplacement [119–121]. Secondly, several complications can arise

due to the catheterization itself, such as severe dysrhythmias, right bundle branch block, or complete heart block. Minor dysrhythmias occur often during catheter insertion or withdrawal but resolve spontaneously after advancing the catheter through the RV [120]. Lastly, prolonged catheter residence can result in pulmonary artery rupture, pulmonary infarction, or venous thrombosis [6]. Catheter-related infections with the PAC are uncommon and involve the introducer sheath rather than the PAC itself [122]. Increased infection risks are associated with prolonged PAC use, insertion via the internal jugular vein rather than the subclavian vein, and unsterile procedures [122, 123]. Right heart catheterizations performed in experienced centres are associated with low risk of serious complications, and there is high quality evidence that PAC use does not alter mortality [6, 124]. Absolute contraindications of PAC placement are right-heart-sided endocarditis, tumours, or masses. Relative contraindications for PAC placement include severe coagulopathy including severe thrombocytopenia, presence of a tricuspid or pulmonary valve prosthesis, new pacing lead, and large atrial septal defect. PAC insertion in patients with a left bundle branch block may induce complete heart block. In patients with TR, catheter passage might be more difficult [125]. Clearly, contraindications related to central venous cannulation, including skin infections and thrombosis of the selected vein, apply to PAC insertion as well.

## 9 Conclusion

The contemporary PAC provides accurate and continuous measurements of CO, RV performance, and of the balance between $DO_2$ and $VO_2$. It provides a multi-variable integration of hemodynamic data in daily clinical practice. Thorough understanding of these PAC-derived measurements and its limitations are key to the successful application of the PAC in clinical practice.

**Supplementary Information** The online version contains supplementary material available at https://doi.org/10.1007/s10877-021-00673-5.

**Authors' contributions** All authors contributed to the design of the review. Literature search and data analysis was performed by ITB. The first draft of the manuscript was written by ITB. All authors critically revised the review. All authors read and approved the final manuscript.

### Compliance with Ethical Standards

**Conflict of interest** ITB, ECB, and FdL do hereby declare that there are no conflict of interest. TWLS received research grants and honoraria from Edwards Lifesciences (Irvine, CA, USA) and Masimo Inc. (Irvine, CA, USA) for consulting and lecturing and from Pulsion Medical Systems SE (Feldkirchen, Germany) for lecturing. TWLS is Editor-in-chief of the Journal of Clinical Monitoring and Computing but had no role in the handling of this manuscript.

**Ethical approval** Not applicable.

**Informed consent** Not applicable.



## References

1. Gnaegi A, Feihl F, Perret C. Intensive care physicians' insufficient knowledge of right-heart catheterization at the bedside: time to act? Crit Care Med. 1997;25(2):213–20.
2. Iberti TJ, Fischer EP, Leibowitz AB, Panacek EA, Silverstein JH, Albertson TE. A multicenter study of physicians' knowledge of the pulmonary artery catheter. Pulmonary Artery Catheter Study Group. JAMA. 1990;264(22):2928–32.
3. Bootsma IT, Boerma EC, de Lange F, Scheeren TWL. The contemporary pulmonary artery catheter. Part 1: placement and waveform analysis. J Clin Monit Comput 2021. https://doi.org/10.1007/s10877-021-00662-8
4. McGee WT, Young C, Frazier JA, editors. Edwards Clinical Education Quick Guide to Cardiopulmonary Care. 4th ed. Irvine: Edwards Critical Care Education; 2018.
5. Marino PL. Marino's the ICU Book. 4th ed. Philadelphia: Lippincott Williams and Wilkins; 2013.
6. Rajaram SS, Desai NK, Kalra A, Gajera M, Cavanaugh SK, Brampton W, *et al*. Pulmonary artery catheters for adult patients in intensive care. Cochrane Database Syst Rev. 2013;2013(2):CD003408.
7. Nishikawa T, Dohi S. Errors in the measurement of cardiac output by thermodilution. Can J Anaesth. 1993;40(2):142–53.
8. Renner LE, Morton MJ, Sakuma GY. Indicator amount, temperature, and intrinsic cardiac output affect thermodilution cardiac output accuracy and reproducibility. Crit Care Med. 1993;21(4):586–97.
9. Nadeau S, Noble WH. Limitations of cardiac output measurements by thermodilution. Can Anaesth Soc J. 1986;33(6):780–4.
10. Argueta EE, Paniagua D. Thermodilution cardiac output: a concept over 250 years in the making. Cardiol Rev. 2019;27(3):138–44.
11. Kubo SH, Burchenal JE, Cody RJ. Comparison of direct fick and thermodilution cardiac output techniques at high flow rates. Am J Cardiol. 1987;59(4):384–6.
12. Thrush DN, Varlotta D. Thermodilution cardiac output: comparison between automated and manual injection of indicator. J Cardiothorac Vasc Anesth. 1992;6(1):17–9.
13. McKenzie SC, Dunster K, Chan W, Brown MR, Platts DG, Javorsky G, *et al*. Reliability of thermodilution derived cardiac output with different operator characteristics. J Clin Monit Comput. 2018;32(2):227–34.

14. Bogaard JM, van Duyl WA, Versprille A, Wise ME. Influence of random noise on the accuracy of the indicator-dilution method. Clin Phys Physiol Meas. 1985;6(1):59–64.
15. Normann RA, Johnson RW, Messinger JE, Sohrab B. A continuous cardiac output computer based on thermodilution principles. Ann Biomed Eng. 1989;17(1):61–73.
16. Yelderman M. Continuous measurement of cardiac output with the use of stochastic system identification techniques. J Clin Monit. 1990;6(4):322–32.
17. Medin DL, Brown DT, Wesley R, Cunnion RE, Ognibene FP. Validation of continuous thermodilution cardiac output in critically ill patients with analysis of systematic errors. J Crit Care. 1998;13(4):184–9.
18. Yelderman ML, Ramsay MA, Quinn MD, Paulsen AW, McKown RC, Gillman PH. Continuous thermodilution cardiac output measurement in intensive care unit patients. J Cardiothorac Vasc Anesth. 1992;6(3):270–4.
19. Sun Q, Rogiers P, Pauwels D, Vincent JL. Comparison of continuous thermodilution and bolus cardiac output measurements in septic shock. Intensive Care Med. 2002;28(9):1276–80.
20. Böttiger BW, Sinner B, Motsch J, Bach A, Bauer H, Martin E. Continuous versus intermittent thermodilution cardiac output measurement during orthotopic liver transplantation. Anaesthesia. 1997;52(3):207–14.
21. Botero M, Kirby D, Lobato EB, Staples ED, Gravenstein N. Measurement of cardiac output before and after cardiopulmonary bypass: comparison among aortic transit-time ultrasound, thermodilution, and noninvasive partial CO2 rebreathing. J Cardiothorac Vasc Anesth. 2004;18(5):563–72.
22. Hogue CW, Rosenbloom M, McCawley C, Lappas DG. Comparison of cardiac output measurement by continuous thermodilution with electromagnetometry in adult cardiac surgical patients. J Cardiothorac Vasc Anesth. 1994;8(6):631–5.
23. Jacquet L, Hanique G, Glorieux D, Matte P, Goenen M. Analysis of the accuracy of continuous thermodilution cardiac output measurement. Comparison with intermittent thermodilution and Fick cardiac output measurement. Intensive Care Med. 1996;22(10):1125–9.
24. Mihaljevic T, von Segesser LK, Tönz M, Leskosek B, Seifert B, Jenni R, *et al*. Continuous versus bolus thermodilution cardiac output measurements—a comparative study. Crit Care Med. 1995;23(5):944–9.
25. Thrush D, Downs JB, Smith RA. Continuous thermodilution cardiac output: agreement with Fick and bolus thermodilution methods. J Cardiothorac Vasc Anesth. 1995;9(4):399–404.
26. Le Tulzo Y, Belghith M, Seguin P, Dall'Ava J, Monchi M, Thomas R, *et al*. Reproducibility of thermodilution cardiac output determination in critically ill patients: comparison between bolus and continuous method. J Clin Monit. 1996;12(5):379–85.
27. Yelderman M, Quinn MD, McKown RC, Eberhart RC, Dollar ML. Continuous thermodilution cardiac output measurement in sheep. J Thorac Cardiovasc Surg. 1992;104(2):315–20.
28. Lazor MA, Pierce ET, Stanley GD, Cass JL, Halpern EF, Bode RH. Evaluation of the accuracy and response time of STAT-mode continuous cardiac output. J Cardiothorac Vasc Anesth. 1997;11(4):432–6.
29. Siegel LC, Hennessy MM, Pearl RG. Delayed time response of the continuous cardiac output pulmonary artery catheter. Anesth Analg. 1996;83(6):1173–7.
30. Nishiwaki C, Kotake Y, Yamada T, Nagata H, Tagawa M, Takeda J. Response time of different methods of cardiac output monitoring during cardiopulmonary resuscitation and recovery. J Cardiothorac Vasc Anesth. 2010;24(2):306–8.
31. Boerboom LE, Kinney TE, Olinger GN, Hoffmann RG. Validity of cardiac output measurement by the thermodilution method in the presence of acute tricuspid regurgitation. J Thorac Cardiovasc Surg. 1993;106(4):636–42.
32. Cigarroa RG, Lange RA, Williams RH, Bedotto JB, Hillis LD. Underestimation of cardiac output by thermodilution in patients with tricuspid regurgitation. Am J Med. 1989;86(4):417–20.
33. Balik M, Pachl J, Hendl J, Martin B, Jan P, Jan H. Effect of the degree of tricuspid regurgitation on cardiac output measurements by thermodilution. Intensive Care Med. 2002;28(8):1117–21.
34. Hoeper MM, Maier R, Tongers J, Niedermeyer J, Hohlfeld JM, Hamm M, *et al*. Determination of cardiac output by the Fick method, thermodilution, and acetylene rebreathing in pulmonary hypertension. Am J Respir Crit Care Med. 1999;160(2):535–41.
35. Buffington CW, Nystrom EUM. Neither the accuracy nor the precision of thermal dilution cardiac output measurements is altered by acute tricuspid regurgitation in pigs. Anesth Analg. 2004;98(4):884–90
36. Griffin K, Benjamin E, DelGiudice R, Schechter C, Iberti TJ. Thermodilution cardiac output measurement during simultaneous volume infusion through the venous infusion port of the pulmonary artery catheter. J Cardiothorac Vasc Anesth. 1997;11(4):437–9.
37. Wetzel RC, Latson TW. Major errors in thermodilution cardiac output measurement during rapid volume infusion. Anesthesiology. 1985;62(5):684–7.
38. Haller M, Zöllner C, Briegel J, Forst H. Evaluation of a new continuous thermodilution cardiac output monitor in critically ill patients: a prospective criterion standard study. Crit Care Med. 1995;23(5):860–6.
39. Ameloot K, Meex I, Genbrugge C, Jans F, Malbrain M, Mullens W, *et al*. Accuracy of continuous thermodilution cardiac output monitoring by pulmonary artery catheter during therapeutic hypothermia in post-cardiac arrest patients. Resuscitation. 2014;85(9):1263–8.
40. Böttiger BW, Rauch H, Böhrer H, Motsch J, Soder M, Fleischer F, *et al*. Continuous versus intermittent cardiac output measurement in cardiac surgical patients undergoing hypothermic cardiopulmonary bypass. J Cardiothorac Vasc Anesth. 1995;9(4):405–11.
41. Neto EP, Piriou V, Durand PG, Du Gres B, Lehot JJ. Comparison of two semicontinuous cardiac output pulmonary artery catheters after valvular surgery. Crit Care Med. 1999;27(12):2694–7.
42. Urban P, Scheidegger D, Gabathuler J, Rutishauser W. Thermodilution determination of right ventricular volume and ejection fraction: a comparison with biplane angiography. Crit Care Med. 1987;15(7):652–5.
43. De Simone R, Wolf I, Mottl-Link S, Böttiger BW, Rauch H, Meinzer HP, *et al*. Intraoperative assessment of right ventricular volume and function. Eur J Cardiothorac Surg. 2005;27(6):988–93.
44. Voelker W, Gruber HP, Ickrath O, Unterberg R, Karsch KR. Determination of right ventricular ejection fraction by thermodilution technique–a comparison to biplane cineventriculography. Intensive Care Med. 1988;14(Suppl 2):461–6.
45. Zink W, Nöll J, Rauch H, Bauer H, Desimone R, Martin E, *et al*. Continuous assessment of right ventricular ejection fraction: new pulmonary artery catheter versus transoesophageal echocardiography. Anaesthesia. 2004;59(11):1126–32.
46. Wiesenack C, Fiegl C, Keyser A, Laule S, Prasser C, Keyl C. Continuously assessed right ventricular end-diastolic volume as a marker of cardiac preload and fluid responsiveness in mechanically ventilated cardiac surgical patients. Crit Care. 2005;9(3):R226–33.
47. Ferris SE, Konno M. In vitro validation of a thermodilution right ventricular ejection fraction method. J Clin Monit. 1992;8(1):74–80.
48. Santamore WP, Gefen N, Avramovich A, Berger P, Kashem A, Barnea O. Right atrial effects on right ventricular ejection

fraction derived from thermodilution measurements. J Cardiothorac Vasc Anesth. 2007;21(5):644–9.
49. Barthélémy R, Roy X, Javanainen T, Mebazaa A, Chousterman BG. Comparison of echocardiographic indices of right ventricular systolic function and ejection fraction obtained with continuous thermodilution in critically ill patients. Crit Care. 2019;23(1):312.
50. Hoeper MM, Tongers J, Leppert A, Baus S, Maier R, Lotz J. Evaluation of right ventricular performance with a right ventricular ejection fraction thermodilution catheter and MRI in patients with pulmonary hypertension. Chest. 2001;120(2):502–7.
51. Starling RC, Binkley PF, Haas GJ, Hatton PS, Wooding-Scott M. Thermodilution measures of right ventricular ejection fraction and volumes in heart transplant recipients: a comparison with radionuclide angiography. J Heart Lung Transplant. 1992;11(6):1140–6.
52. Fredriksson AG, Zajac J, Eriksson J, Dyverfeldt P, Bolger AF, Ebbers T, *et al*. 4-D blood flow in the human right ventricle. Am J Physiol Heart Circ Physiol. 2011;301(6):H2344–50.
53. Durham R, Neunaber K, Vogler G, Shapiro M, Mazuski J. Right ventricular end-diastolic volume as a measure of preload. J Trauma. 1995;39(2):218–3; discussion 223.
54. Nelson LD, Safcsak K, Cheatham ML, Block EF. Mathematical coupling does not explain the relationship between right ventricular end-diastolic volume and cardiac output. Crit Care Med. 2001;29(5):940–3.
55. Chang MC, Black CS, Meredith JW. Volumetric assessment of preload in trauma patients: addressing the problem of mathematical coupling. Shock. 1996;6(5):326–9.
56. Armaganidis A, Dhainaut JF, Billard JL, Klouche K, Mira JP, Brunet F, *et al*. Accuracy assessment for three fiberoptic pulmonary artery catheters for $SvO_2$ monitoring. Intensive Care Med. 1994;20(7):484–8.
57. Marik PE, Cavallazzi R. Does the central venous pressure predict fluid responsiveness? An updated meta-analysis and a plea for some common sense. Crit Care Med. 2013;41(7):1774–81.
58. Osman D, Ridel C, Ray P, Monnet X, Anguel N, Richard C, *et al*. Cardiac filling pressures are not appropriate to predict hemodynamic response to volume challenge. Crit Care Med. 2007;35(1):64–8.
59. Kumar A, Anel R, Bunnell E, Habet K, Zanotti S, Marshall S, *et al*. Pulmonary artery occlusion pressure and central venous pressure fail to predict ventricular filling volume, cardiac performance, or the response to volume infusion in normal subjects. Crit Care Med. 2004;32(3):691–9.
60. Maughan WL, Shoukas AA, Sagawa K, Weisfeldt ML. Instantaneous pressure-volume relationship of the canine right ventricle. Circ Res. 1979;44(3):309–15.
61. Redington AN, Rigby ML, Shinebourne EA, Oldershaw PJ. Changes in the pressure-volume relation of the right ventricle when its loading conditions are modified. Br Heart J. 1990;63(1):45–9.
62. Alderman EL, Glantz SA. Acute hemodynamic interventions shift the diastolic pressure-volume curve in man. Circulation. 1976;54(4):662–71.
63. Vellinga NA, Ince C, Boerma EC. Elevated central venous pressure is associated with impairment of microcirculatory blood flow in sepsis: a hypothesis generating post hoc analysis. BMC Anesthesiol. 2013;13(1):17.
64. Damman K, van Deursen VM, Navis G, Voors AA, van Veldhuisen DJ, Hillege HL. Increased central venous pressure is associated with impaired renal function and mortality in a broad spectrum of patients with cardiovascular disease. J Am Coll Cardiol. 2009;53(7):582–8.
65. van Deursen VM, Damman K, Hillege HL, van Beek AP, van Veldhuisen DJ, Voors AA. Abnormal liver function in relation to hemodynamic profile in heart failure patients. J Card Fail. 2010;16(1):84–90.
66. Pinsky MR, Kellum JA, Bellomo R. Central venous pressure is a stopping rule, not a target of fluid resuscitation. Crit Care Resusc. 2014;16(4):245–6.
67. Eskesen TG, Wetterslev M, Perner A. Systematic review including re-analyses of 1148 individual data sets of central venous pressure as a predictor of fluid responsiveness. Intensive Care Med. 2016;42(3):324–32.
68. Guyton AC, Lindsey AW, Abernathy B, Richardson T. Venous return at various right atrial pressures and the normal venous return curve. Am J Physiol. 1957;189(3):609–15.
69. Guyton AC. Determination of cardiac output by equating venous return curves with cardiac response curves. Physiol Rev. 1955;35(1):123–9.
70. Magder S. Bench-to-bedside review: an approach to hemodynamic monitoring–Guyton at the bedside. Crit Care. 2012;16(5):236.
71. Funcke S, Sander M, Goepfert MS, Groesdonk H, Heringlake M, Hirsch J, *et al*. Practice of hemodynamic monitoring and management in German, Austrian, and Swiss intensive care units: the multicenter cross-sectional ICU-CardioMan study. Ann Intensive Care. 2016;6(1):49.
72. Patterson SW, Starling EH. On the mechanical factors which determine the output of the ventricles. J Physiol. 1914;48(5):357–79.
73. Cecconi M, Parsons AK, Rhodes A. What is a fluid challenge? Curr Opin Crit Care. 2011;17(3):290–5.
74. Cecconi M, De Backer D, Antonelli M, Beale R, Bakker J, Hofer C, *et al*. Consensus on circulatory shock and hemodynamic monitoring. Task force of the European Society of Intensive Care Medicine. Intensive Care Med. 2014;40(12):1795–815.
75. Santamore WP, Dell'Italia LJ. Ventricular interdependence: significant left ventricular contributions to right ventricular systolic function. Prog Cardiovasc Dis. 1998;40(4):289–308.
76. Weyman AE, Wann S, Feigenbaum H, Dillon JC. Mechanism of abnormal septal motion in patients with right ventricular volume overload: a cross-sectional echocardiographic study. Circulation. 1976;54(2):179–86.
77. Konstam MA, Kiernan MS, Bernstein D, Bozkurt B, Jacob M, Kapur NK, *et al*. Evaluation and management of right-sided heart failure: a scientific statement from the American Heart Association. Circulation. 2018;137(20):e578-622.
78. Hrymak C, Strumpher J, Jacobsohn E. Acute right ventricle failure in the intensive care unit: assessment and management. Can J Cardiol. 2017;33(1):61–71.
79. Lopez-Sendon J, Coma-Canella I, Gamallo C. Sensitivity and specificity of hemodynamic criteria in the diagnosis of acute right ventricular infarction. Circulation. 1981;64(3):515–25.
80. Haddad F, Doyle R, Murphy DJ, Hunt SA. Right ventricular function in cardiovascular disease, part II: pathophysiology, clinical importance, and management of right ventricular failure. Circulation. 2008;117(13):1717–31.
81. Harjola VP, Mebazaa A, Čelutkienė J, Bettex D, Bueno H, Chioncel O, *et al*. Contemporary management of acute right ventricular failure: a statement from the heart failure association and the working group on pulmonary circulation and right ventricular function of the European Society of Cardiology. Eur J Heart Fail. 2016;18(3):226–41.
82. Bootsma IT, de Lange F, Koopmans M, Haenen J, Boonstra PW, Symersky T, *et al*. Right ventricular function after cardiac surgery is a strong independent predictor for long-term mortality. J Cardiothorac Vasc Anesth. 2017;31(5):1656–62.
83. Winkelhorst JC, Bootsma IT, Koetsier PM, de Lange F, Boerma EC. Right ventricular function and long-term outcome in sepsis: a retrospective cohort study. Shock. 2020;53(5):537–43.

84. Bellofiore A, Chesler NC. Methods for measuring right ventricular function and hemodynamic coupling with the pulmonary vasculature. Ann Biomed Eng. 2013;41(7):1384–98.
85. Naeije R, Badagliacca R. The overloaded right heart and ventricular interdependence. Cardiovasc Res. 2017;113(12):1474–85.
86. Lim HS, Gustafsson F. Pulmonary artery pulsatility index: physiological basis and clinical application. Eur J Heart Fail. 2020;22(1):32–8.
87. Mehmood M, Biederman RWW, Markert RJ, McCarthy MC, Tchorz KM. Right heart function in critically Ill patients at risk for acute right heart failure: a description of right ventricular-pulmonary arterial coupling, ejection fraction and pulmonary artery pulsatility index. Heart Lung Circ. 2020;29(6):867–73.
88. Grønlykke L, Couture EJ, Haddad F, Amsallem M, Ravn HB, Raymond M, *et al*. Preliminary experience using diastolic right ventricular pressure gradient monitoring in cardiac surgery. J Cardiothorac Vasc Anesth. 2020;34(8):2116–25.
89. Denault AY, Chaput M, Couture P, Hébert Y, Haddad F, Tardif JC. Dynamic right ventricular outflow tract obstruction in cardiac surgery. J Thorac Cardiovasc Surg. 2006;132(1):43–9.
90. Raymond M, Grønlykke L, Couture EJ, Desjardins G, Cogan J, Cloutier J, *et al*. Perioperative right ventricular pressure monitoring in cardiac surgery. J Cardiothorac Vasc Anesth. 2019;33(4):1090–104.
91. Stevenson LW, Perloff JK. The limited reliability of physical signs for estimating hemodynamics in chronic heart failure. JAMA. 1989;261(6):884–8.
92. Rossello X, Vila M, Rivas-Lasarte M, Ferrero-Gregori A, Sans-Roselló J, Duran-Cambra A, *et al*. Impact of pulmonary artery catheter use on short- and long-term mortality in patients with cardiogenic shock. Cardiology. 2017;136(1):61–9.
93. Frost AE, Farber HW, Barst RJ, Miller DP, Elliott CG, McGoon MD. Demographics and outcomes of patients diagnosed with pulmonary hypertension with pulmonary capillary wedge pressures 16 to 18 mm Hg: insights from the REVEAL Registry. Chest. 2013;143(1):185–95.
94. Halpern SD, Taichman DB. Misclassification of pulmonary hypertension due to reliance on pulmonary capillary wedge pressure rather than left ventricular end-diastolic pressure. Chest. 2009;136(1):37–43.
95. Freed MD, Miettinen OS, Nadas AS. Oximetric detection of intracardiac left-to-right shunts. Br Heart J. 1979;42(6):690–4.
96. Buda AJ, Pinsky MR, Ingels NB, Daughters GT, Stinson EB, Alderman EL. Effect of intrathoracic pressure on left ventricular performance. N Engl J Med. 1979;301(9):453–9.
97. Lamia B, Maizel J, Ochagavia A, Chemla D, Osman D, Richard C, *et al*. Echocardiographic diagnosis of pulmonary artery occlusion pressure elevation during weaning from mechanical ventilation. Crit Care Med. 2009;37(5):1696–701.
98. Lessard MR, Lofaso F, Brochard L. Expiratory muscle activity increases intrinsic positive end-expiratory pressure independently of dynamic hyperinflation in mechanically ventilated patients. Am J Respir Crit Care Med. 1995;151(2 Pt 1):562–9.
99. Butler J, Schrijen F, Henriquez A, Polu JM, Albert RK. Cause of the raised wedge pressure on exercise in chronic obstructive pulmonary disease. Am Rev Respir Dis. 1988;138(2):350–4.
100. Lemaire F, Teboul JL, Cinotti L, Giotto G, Abrouk F, Steg G, *et al*. Acute left ventricular dysfunction during unsuccessful weaning from mechanical ventilation. Anesthesiology. 1988;69(2):171–9.
101. Jubran A, Mathru M, Dries D, Tobin MJ. Continuous recordings of mixed venous oxygen saturation during weaning from mechanical ventilation and the ramifications thereof. Am J Respir Crit Care Med. 1998;158(6):1763–9.
102. Alía I, Esteban A. Weaning from mechanical ventilation. Crit Care. 2000;4(2):72–80.
103. Cabello B, Thille AW, Roche-Campo F, Brochard L, Gómez FJ, Mancebo J. Physiological comparison of three spontaneous breathing trials in difficult-to-wean patients. Intensive Care Med. 2010;36(7):1171–9.
104. Hoeper MM, Bogaard HJ, Condliffe R, Frantz R, Khanna D, Kurzyna M, *et al*. Definitions and diagnosis of pulmonary hypertension. J Am Coll Cardiol. 2013;62(25 Suppl):D42-50.
105. Galiè N, Humbert M, Vachiery JL, Gibbs S, Lang I, Torbicki A, *et al*. 2015 ESC/ERS guidelines for the diagnosis and treatment of pulmonary hypertension: the joint task force for the diagnosis and treatment of pulmonary hypertension of the European Society of Cardiology (ESC) and the European Respiratory Society (ERS): Endorsed by: Association for European Paediatric and Congenital Cardiology (AEPC), International Society for Heart and Lung Transplantation (ISHLT). Eur Heart J. 2016;37(1):67–119.
106. Simonneau G, Montani D, Celermajer DS, Denton CP, Gatzoulis MA, Krowka M, *et al*. Haemodynamic definitions and updated clinical classification of pulmonary hypertension. Eur Respirat J. 2019;53(1):1801913.
107. Deaño RC, Glassner-Kolmin C, Rubenfire M, Frost A, Visovatti S, McLaughlin VV, *et al*. Referral of patients with pulmonary hypertension diagnoses to tertiary pulmonary hypertension centers: the multicenter RePHerral study. JAMA internal Med. 2013;173(10):887–93.
108. Gayat E, Mebazaa A. Pulmonary hypertension in critical care. Curr Opin Crit Care. 2011;17(5):439–48.
109. Vieillard-Baron A, Schmitt JM, Augarde R, Fellahi JL, Prin S, Page B, *et al*. Acute cor pulmonale in acute respiratory distress syndrome submitted to protective ventilation: incidence, clinical implications, and prognosis. Crit Care Med. 2001;29(8):1551–5.
110. Tsapenko MV, Tsapenko AV, Comfere TB, Mour GK, Mankad SV, Gajic O. Arterial pulmonary hypertension in noncardiac intensive care unit. Vasc Health Risk Manag. 2008;4(5):1043–60.
111. Vlahakes GJ, Turley K, Hoffman JI. The pathophysiology of failure in acute right ventricular hypertension: hemodynamic and biochemical correlations. Circulation. 1981;63(1):87–95.
112. Naeije R, Vanderpool R, Peacock A, Badagliacca R. The right heart-pulmonary circulation unit: physiopathology. Heart Fail Clin. 2018;14(3):237–45.
113. Mark JB. Pericardial Constriction and Cardiac Tamponade. Atlas of Cardiovascular Monitoring. New York: Churchill Livingstone; 1988. p. 313–26.
114. Kearns MJ, Walley KR. Tamponade: hemodynamic and echocardiographic diagnosis. Chest. 2018;153(5):1266–75.
115. Teboul JL, Saugel B, Cecconi M, De Backer D, Hofer CK, Monnet X, *et al*. Less invasive hemodynamic monitoring in critically ill patients. Intensive Care Med. 2016;42(9):1350–9.
116. Robitaille A, Denault AY, Couture P, Bélisle S, Fortier A, Guertin MC, *et al*. Importance of relative pulmonary hypertension in cardiac surgery: the mean systemic-to-pulmonary artery pressure ratio. J Cardiothorac Vasc Anesth. 2006;20(3):331–9.
117. Saydain G, Awan A, Manickam P, Kleinow P, Badr S. Pulmonary hypertension an independent risk factor for death in intensive care unit: correlation of hemodynamic factors with mortality. Clinical medicine insights. Circ Respir Pulm Med. 2015;9:27–33.
118. Lim HS. Cardiac power output revisited. Circ Heart Fail. 2020;13(10):e007393.
119. Lamperti M, Bodenham AR, Pittiruti M, Blaivas M, Augoustides JG, Elbarbary M, *et al*. International evidence-based recommendations on ultrasound-guided vascular access. Intensive Care Med. 2012;38(7):1105–17.
120. American Society of Anesthesiologists Task Force on Pulmonary Artery Catheterization. Practice guidelines for pulmonary artery catheterization: an updated report by the American Society of

Anesthesiologists Task Force on Pulmonary Artery Catheterization. Anesthesiology. 2003;99(4):988–1014.
121. Saugel B, Scheeren TWL, Teboul JL. Ultrasound-guided central venous catheter placement: a structured review and recommendations for clinical practice. Crit Care. 2017;21(1):225.
122. Cohen Y, Fosse JP, Karoubi P, Reboul-Marty J, Dreyfuss D, Hoang P, *et al*. The "hands-off" catheter and the prevention of systemic infections associated with pulmonary artery catheter: a prospective study. Am J Respir Crit Care Med. 1998;157(1):284–7.
123. Mermel LA, McCormick RD, Springman SR, Maki DG. The pathogenesis and epidemiology of catheter-related infection with pulmonary artery Swan-Ganz catheters: a prospective study utilizing molecular subtyping. Am J Med. 1991;91(3B):197S-205S.
124. Hoeper MM, Lee SH, Voswinckel R, Palazzini M, Jais X, Marinelli A, *et al*. Complications of right heart catheterization procedures in patients with pulmonary hypertension in experienced centers. J Am Coll Cardiol. 2006;48(12):2546–52.
125. Kelly CR, Rabbani LE. Videos in clinical medicine. Pulmonary-artery catheterization. N Engl J Med. 2013;369(25):e35.